Geospatial approach for assessing spatiotemporal dynamics of urban green space distribution among neighbourhoods: A demonstration in Mumbai.

Abstract

Green spaces are an integral part of urban landscape and offer numerous benefits related to quality of urban life. However, due to various factors, the distribution of green spaces among city neighbourhoods is often skewed. Hence, urban planners require effective tools to routinely map and monitor the greening/ un-greening phenomena among the neighbourhoods. This study caters to this need by adopting a novel geospatial green space distribution assessment approach that encompasses green space quantity, quality and accessibility aspects. The green space distribution indicators were derived from remote sensing data, which facilitates cost-effective green space assessments at desired time scales. Further, the approach includes a statistical design to identify the hotspots of green space augmentation/degradation using local Moran's I, an index of spatial autocorrelation. In this study, the approach is demonstrated in Mumbai, a typical city in a developing country undergoing urbanization transition accompanied by stark environmental challenges. The study results revealed that the green spaces in Mumbai had generally diminished, fragmented and disaggregated between 2001 and 2011. However, the level of degeneration of green spaces was found to vary significantly among the neighbourhoods. Statistical analyses unveiled that the verdant spaces in the city's western suburbs had experienced the worst degradation during the study period. These results would aid Mumbai's planners in formulating local greening strategies in a cost-effective manner. Further, the study has wider implications for green space planning, especially in the understudied, fast-urbanizing developing countries.

Keywords: Urban environment, compact city, remote sensing, spatial metrics, spatial autocorrelation, India.

Research Highlights

- Green space quantity, quality and accessibility assessed using remote sensing data.
- Mumbai lost 22.6% of its green space area between 2001 and 2011.
- The city’s green spaces largely turned smaller, fragmented and disaggregated.
- Rise in per capita green space in few neighbourhoods due to decreasing population.
- Degeneration of green spaces was focused mainly in the western suburbs.

1. Introduction

Urban green spaces refer to all open spaces within city limits covered with vegetation by design or default (*Lo and Jim, 2012*). They include parks, gardens, and even the informal vegetated spaces in derelict public and private lands, historical places, abandoned industrial sites, and along transportation and utility corridors (*Gupta et al., 2012; Anguluri and Narayanan, 2017).* These green spaces form an integral part of urban landscape as they enhance quality of urban life in several aspects. They provide ecosystem services, preserve biodiversity, promote public health, encourage social interaction, influence property pricings, and also mitigate the urban heat island (UHI) effect (*Gupta et al., 2012; O'Malley et al., 2015; De la Barrera et al., 2016a; Mehrotra et al., 2019).* For effective utilization of these benefits, green spaces must be available in and near the places where people live, work and play (*Lin et al., 2015)*. However, the distribution of green spaces among city neighbourhoods is often skewed, due to various socio-economic and cultural factors (*Pham et al., 2012; Zhou and Kim, 2013; Li and Liu, 2016*). Spatial imbalances in provision of green spaces and the associated benefits is a recognized environmental justice issue worldwide (*Heynen et al., 2006; Rigolon et al., 2018*), which warrants periodic checks and counter measures. By conducting routine neighbourhood-level green space distribution assessments, city planners can discover the spatiotemporal trends in greening or un-greening, and thereby design localized strategies to improve the efficacy of their greening efforts.

The need for green space assessments at neighbourhood level is particularly exigent for the developing countries, which will house 80% of world urban population by 2030 (*UNPF, 2007*). Inadequate green space planning coupled with degrading environmental quality calls for a green space agenda in these cities (*Senanayake et al., 2013; De la Barrera et al., 2016a*). However, much of the relevant literature on green space distribution assessment are focussed in the developed countries (*Kabisch et al., 2015*). As key drivers of urban growth in the developed and developing countries are markedly different, a significant knowledge gap exists on urban green space inventory, and characteristics of spatial inequities in green space distribution in cities of the Global South (*Bardhan et al., 2016; Fernandez and Wu, 2016*). The difficulty in addressing this gap is intensified by the fact that in these countries urban growth is largely informal and planners are mostly under-resourced (*Pethe et al., 2014; De Satge and Watson, 2018*). Hence, quality information on urban green space distribution among city neighbourhoods at desired time scales is often lacking in these countries. This challenge, however, can be overcome by means of remote sensing data. Compared to the resource intensive traditional ground surveys, remote sensing offers a cost-effective alternative to conduct synoptic and repetitive monitoring of green spaces in a short span of time (*Maktav et al., 2005*; *Franco and Macdonald, 2017*).

Although a few prior studies have presented remote sensing-based approaches to assess neighbourhood level urban green space distribution in developing countries, there are several methodological and practical issues that hamper conducting periodic assessments. Most studies used only quantity measures such as percentage of green space area or green space area per resident (e.g., *Senanayake et al., 2013; Anguluri and Narayanan, 2017; Nero, 2017; Singh, 2018; Shekhar and Aryal, 2019*). However, in addition to quantity, quality and accessibility of green spaces also influence the benefits offered to the residents and, hence, are key attributes in green space assessments (*Yao et al., 2014; Haaland and van den Bosch, 2015; De la Barrera et al., 2016b*). *Gupta et al. (2012)* proposed an Urban Neighbourhood Green Index (UNGI) to assess green space quality based on green space quantity, proximity to green spaces, built-up density and height of buildings derived from high resolution satellite images. However, estimating the height of buildings across a city using high resolution images incurs huge acquisition and processing costs, thus rendering the method unfeasible for periodic assessments in developing countries. Further, some studies that included accessibility aspect of green spaces generally considered the total population of blocks falling within a certain distance threshold from green spaces as accessibility measure (e.g., *Li and Liu, 2016; You, 2016; De la Barrera et al., 2016b*). However, block-level population data is seldom available in most developing countries such as India (*Baud et al., 2010*).

Recent studies indicate that quality and accessibility of green spaces are closely linked to their size, shape and other configurational aspects. For example, large and well-connected green spaces support more biodiversity, large social gatherings, simultaneous multiple uses, and hence offer high quality (*Wright Wendel et al., 2012; De la Barrera et al., 2016b*). Similarly, elongated and well-distributed green space patches attract and benefit more number of residents (*Jim, 2013; Tian et al., 2014*). Therefore, configurational aspects can serve as indicators of neighbourhood-level green space quality (*Li and Liu, 2016; You, 2016; De la Barrera et al., 2016b*) and accessibility (*Sathyakumar et al., 2018*). Such configurational aspects of green spaces can also be extracted from remote sensing data, and quantified using spatial metrics (*Qian et al., 2015; Sathyakumar et al., 2018*). Although prior studies on various themes (e.g., *Zhou and Wang, 2011; Qian et al., 2015; Zhou et al., 2018*) have assessed the spatiotemporal changes in green space configuration based on few remote sensing-derived spatial metrics, these changes have not been linked to spatiotemporal dynamics of neighbourhood level green space quality and accessibility.

Furthermore, given the limited resources available for green space planning in developing countries, urban planners need to target greening programs at specific neighbourhoods that critically deserve more attention. Hence, in addition to mapping spatiotemporal variations in green space distribution among city neighbourhoods, planners need to identify the hotspot neighbourhoods of green space augmentation/degradation. However, to the authors' knowledge, no available study presents a statistical design to identify neighbourhood clusters and outliers of green space dynamics that includes quantity, quality and accessibility aspects. Development of such statistical design using remotely sensed indicators of green space distribution at neighbourhood level may greatly facilitate informed green space planning, especially in developing countries.

In view of the above, this study adopts a novel remote sensing-oriented approach to i) analyse spatiotemporal variations in neighbourhood-level urban green space distribution (in terms of quantity, quality and accessibility), and ii) statistically identify hotspots of green space improvement/degeneration, particularly useful for developing countries. For this study, we chose the city of Mumbai, India. Similar to other cities in developing countries, Mumbai is undergoing urbanization transition accompanied by stark environmental and planning challenges (*Pacione, 2006; Pethe et al., 2014*). The green spaces in Mumbai grapple with intense development pressure driven chiefly by economic interests almost on a day-to-day basis (*Zerah, 2007; Shafizadeh Moghadam and Helbich, 2013*). However, the spatiotemporal variations in green spaces among Mumbai's neighbourhoods have not been investigated before. The current study assesses the spatiotemporal dynamics of green space distribution in Mumbai between 2001 and 2011 and maps the hotspots of greening or un-greening phenomena in the city. The study results contribute to the less studied urban green spaces of the developing world in general, and efficient planning and management of green spaces in Mumbai in particular.

2. Study Area

Mumbai is one of the rapidly growing megacities in the world with a population of over 12.4 million in 2011 (*Census PCA, 2011*). The city is located between 18^0 53' and 19^0 17' North latitudes and 72^0 46' and 72^0 59' East longitudes, and lies on a peninsula on the west coast of India. The city is divided into Mumbai City and Mumbai Suburban revenue districts. The suburbs have remained part of the city since the 1950s, and are further divided into Eastern and Western suburbs (Fig. 1). The share of suburban population to the total population is on the rise consistently since 1981, and was more than 75% in 2011 (*MCGM, 2016*). On the other hand, between 2001 and 2011 the population in City District decreased by 0.25 million although Mumbai's population increased by 0.46 million (*MCGM, 2016*). Land use planning and civic administration of the city is carried out by the Municipal Corporation of Greater Mumbai (MCGM), which draws up periodical development plans. However, urban growth in Mumbai is predominantly spontaneous with a mix of residential, commercial and industrial land uses (*Pethe et al., 2014; MCGM, 2016*). For administrative reasons, MCGM has divided the city into 24 wards, which are further divided into 88 census sections (Fig. 1). Census section is the basic unit of population data in Mumbai, and is akin to neighbourhood (*Bardhan et al., 2015b, Sathyakumar et al., 2018*).

The chief constituent of green space in Mumbai is the Sanjay Gandhi National Park (SGNP), which is roughly spread across 100 km^2 in the suburbs. However, the park is subject to continued encroachment despite being declared a no development zone (*Zerah, 2007*). Other green spaces include the mangrove-rich suburbs in northwest and east, and the hill ranges in the eastern suburbs (*Sathyakumar et al., 2018*). Apart from these, a few parks and recreational spaces account for the city's green spaces.

As a major industrial and financial hub, Mumbai attracts migrants, mainly low skilled single adults of poor economic background, from across the country (*Pacione, 2006*). However, due to the exorbitant real estate prices in Mumbai, these migrants mostly settle in informal settlements like slums and *chawls (Bardhan et al., 2015a)*. As a result, above 40% of Mumbai's population in 2011 lived in slums, which are mainly located on the peripheries of natural green spaces like mangroves, hills and forests in the suburbs (*MCGM, 2016*). With Mumbai's population projected to further rise to 12.8 million in 2021, planners are in dire need to conserve existing green spaces as well as develop new ones against development pressure (*MCGM, 2016*).

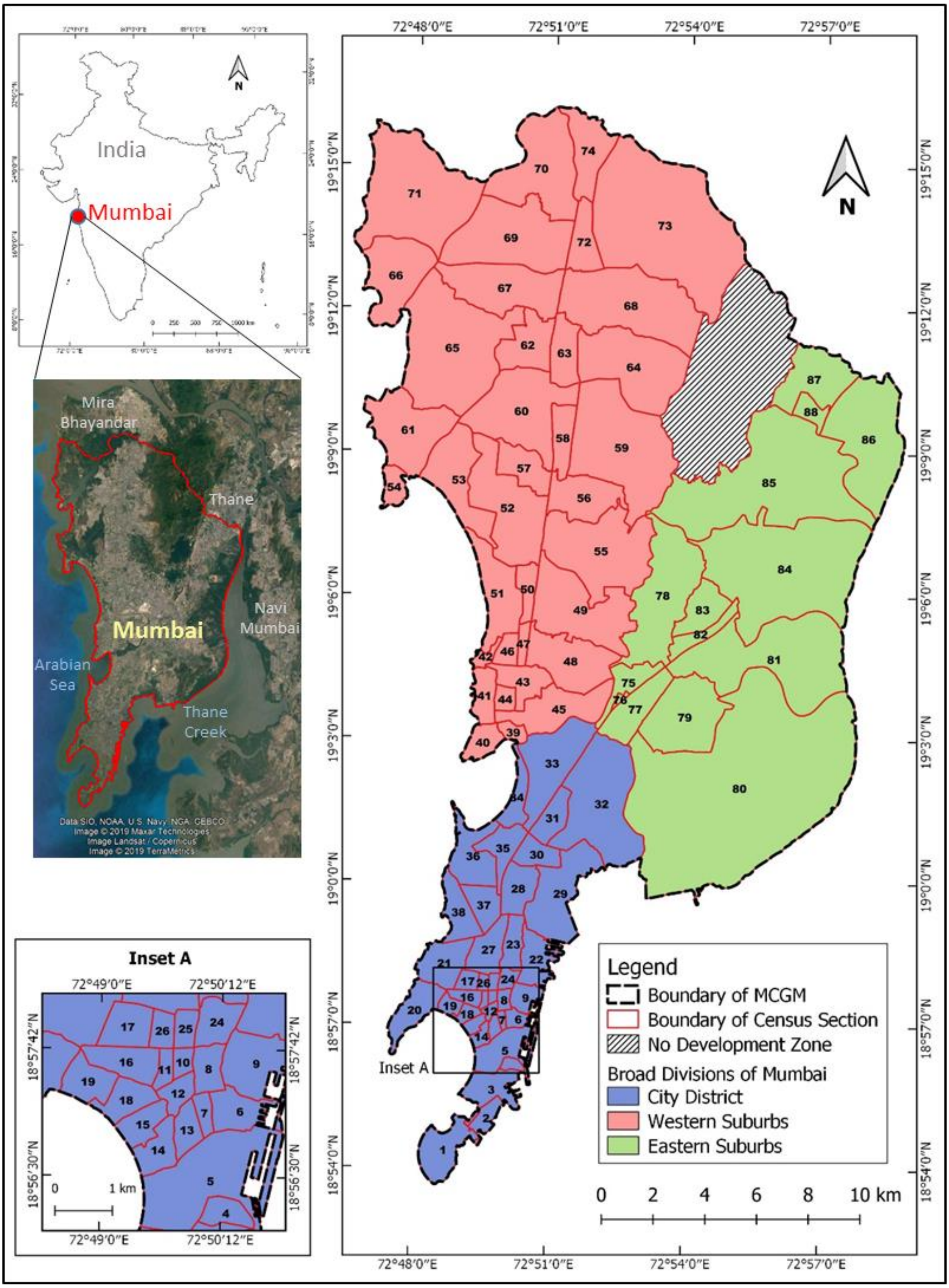

Fig. 1. Map of census sections in Mumbai.
Note: Numbers represent the ID of census sections; Map inset provides enlarged view of a subset of study area.

3. Data and Methods

The study workflow (Fig. 2) involves extraction and comparison of green space distribution in Mumbai at the level of census sections in the latest two census years of 2001 and 2011. ‘Census section’ is a spatial unit defined for census operations within the city, and is the finest level of census data available to the public (*MCGM*, *2016*). Mumbai was split into 88 census sections for Census 2001, and the same were retained for Census 2011.

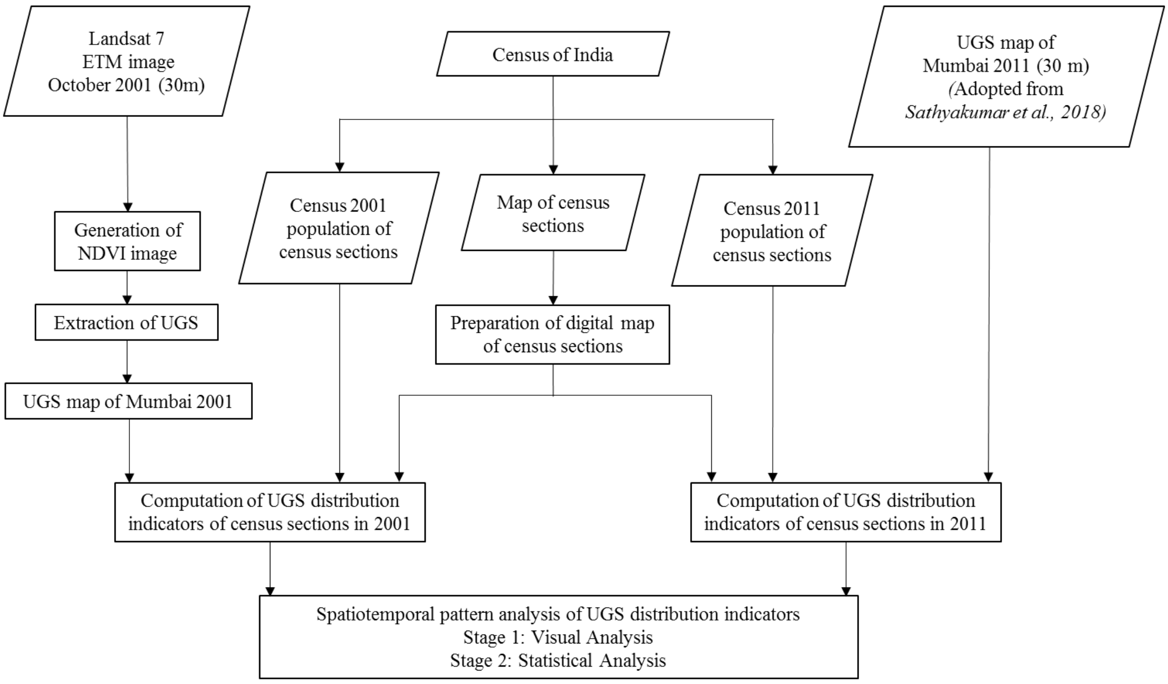

Fig. 2. Methodological framework adopted for the study.

3.1 Data description

In this study, the following data were used: i) Census data- to obtain census section boundaries and population data, ii) Map of urban green spaces in Mumbai in 2011, and iii) Remote sensing data- to extract urban green spaces in Mumbai in 2001.

3.1.1 Census data

A digital map of the census sections in Mumbai is currently not available in the public domain. Hence, a “shapefile” of census sections was created on Geographic Information System (GIS) platform by referring the assembly constituency maps provided online by the

Chief Electoral Officer, Maharashtra (*CEO Maharashtra, 2017*). These online maps also show the census sections in each assembly constituency, and label the roads and railway lines that form the census section boundaries, but do not contain any geographic coordinates. The digitization procedure adopted to create the shapefile is as follows: First, the Google Terrain map of Mumbai was loaded as base layer in QGIS (version 2.14), a GIS package, using the *QuickMapServices* plugin (*QGIS*, 2019; Map Data: Google). Then, the census section boundaries provided in the online maps were identified and traced on the base map in form of a shapefile. This shapefile was then reprojected to match the coordinate system of the green space map of 2011 used in the study (discussed in section 3.1.2). Few minor geometric distortions observed in the shapefile were then corrected using the *Spatial Adjustment* tool (Affine transformation method) in ArcGIS 10.6 software. To assess the data quality of the shapefile, the digitization process was reiterated twice more for selected nine census sections (IDs: 4, 10, 37, 44, 57, 72, 79, 82 and 86). These chosen nine census sections are of varying areas and are geographically distributed across the study region. Based on the area of these census sections, data quality of the shapefile was estimated to have an error of 0.006% ± 0.25% at 99% confidence interval (*Sathyakumar et al., 2018*).

The population data of census sections in 2001 and 2011 were obtained from the final population totals of Census 2001 (*Census FPT, 2001*) and the primary census abstract of Census 2011 (*Census PCA, 2011*) respectively.

3.1.2 Map of urban green spaces in Mumbai in 2011

The map of green spaces in the city in 2011 at 30m spatial resolution was adopted from *Sathyakumar et al. (2018*). This map was prepared using IRS Resourcesat-2 LISS-IV images of 5m spatial resolution that were reduced to 30m spatial resolution using the *Degrade* tool in *ERDAS* Imagine 2014 package. The map accuracy was estimated to be 83.11%, with a 95%

confidence interval of 79.42% to 86.78% (refer section 4.1). More information on the map is available in *Sathyakumar et al. (2018).*

3.1.3 Remote sensing data

To extract the green spaces in the city in 2001, we used Landsat 7 Enhanced Thematic Mapper (ETM) Level 1TP image of Mumbai (path ID-148; row ID-47) acquired on October 25, 2001. The image was downloaded from the website of United States Geological Survey (USGS), and has a spatial resolution of 30m. It contains spectral reflectances in red (0.63-0.69µm) and near infrared (0.75-0.90µm) bands, which are useful for vegetation mapping. This image was chosen as its date of acquisition conforms to the same season (post-monsoon) when the LISS-IV images used to generate the green space map of 2011 were acquired (*Sathyakumar et al., 2018*). Due to seasonal homogeneity, the potential effects of seasonal variations on the mapping of green spaces in both years were limited. Further, the spatial resolution of this image (30m) matches that of the green spaces map of 2011 used in this study. Maintaining a uniform spatial resolution is critical to this multi-temporal study as the spatial metrics characterizing green space distribution (discussed in section 3.2.4) are susceptible to the effects of changing scales (*Shen et al., 2004; Buyantuyev et al., 2010; Sathyakumar et al., 2018*).

3.2 Methodology

3.2.1 Preprocessing of remote sensing data

Geometric distortions were observed between the ETM image of 2001 and the urban green space map of 2011. Hence, the ETM image was co-registered with the degraded LISS-IV images (30m) used to generate the green space map of 2011, using the *Georeferencing Wizard* (Affine geometric model) of ERDAS Imagine 2014. As the root mean square error obtained was within 0.5 pixels, the corrected ETM image was used for further analysis.

3.2.2 Extraction of urban green spaces

A universal definition of urban green spaces is still lacking. However, this study adopted the commonly followed definition that considers all vegetated areas within city limits as urban green spaces (*Lo and Jim, 2012; Taylor and Hochuli, 2017*). Accordingly, the urban green spaces in Mumbai in 2001 was extracted using the Normalized Difference Vegetation Index (NDVI) method (*Gupta et al., 2012; Senanayake et al., 2013; Nero, 2017; Sathyakumar et al., 2018*). NDVI, a commonly used vegetation index, uses spectral reflectances in the red (R) and near infrared (NIR) bands of multispectral remote sensing data to measure vegetation intensity (*Gascon et al., 2016*). The index is given as (NIR-R)/(NIR+R) and varies from -1 to +1, with vegetation pixels typically taking values greater than 0.2 (*Franco and Macdonald, 2017*).

Radiometric corrections were performed to convert the ETM image from digital numbers (DN) to top of atmosphere spectral reflectances, and the corresponding NDVI image was generated. While previous studies (e.g., *Nero, 2017; Senanayake et al., 2013*) relied either on simple arbitrary NDVI threshold or on visual comparison to determine the NDVI threshold defining green and non-green pixels, in this study the threshold was objectively determined using Otsu threshold selection method (*Otsu, 1979; Sathyakumar et al., 2018*) in MATLAB. Otsu method evaluates a criterion function based on the between-class variance and total variance for all possible threshold values; the value that maximizes the criterion function is considered the optimal threshold (*Sunder et al., 2017*). Accordingly, a suitable NDVI threshold was obtained and used to create binary images containing vegetation and non-vegetation pixels. This binary image constituted the map of urban green spaces in Mumbai in 2001. This map has a spatial resolution of 30m and includes all green spaces in Mumbai regardless of ownership or access, in accordance with the adopted definition of urban green spaces (*Lo and Jim, 2012; Zhou et al., 2018; Du Toit et al., 2018*).

3.2.3 Accuracy assessment of urban green space maps

Accuracy of the two urban green space maps used in the study was assessed based on the format recommended by *Stehman and Foody (2019).* This format recommends an error matrix expressed in terms of percentage of area of each map class, rather than the conventional error matrix comprised of sample counts. Also, this format recommends reporting the standard errors associated with the accuracy estimates as a requirement for statistically rigorous accuracy assessment.

For assessing the accuracy of the two green space maps, a total of 400 random points distributed across the study area were chosen. The sample size was chosen based on a conservative overall accuracy target of 50%, a confidence interval of 95%, and a desired confidence interval half-width of 5% (*Stehman and Foody, 2019*). Reference data were collected from Google Earth images of the respective years and through visual interpretation of the satellite images. Based on the collected reference data, the overall accuracies of the maps were computed along with their 95% confidence interval estimates (as suggested by *Stehman and Foody, 2019*).

3.2.4 Computation of urban green space distribution indicators

Recent studies have recommended incorporating quantity, quality and accessibility aspects for a comprehensive assessment of urban green space distribution (*Yao et al., 2014; Tian et al., 2014; De la Barrera et al., 2016b*). Accordingly, this study adopted seven urban green spaces (UGS) distribution indicators (Table 1). Among these, the two indicators- Percentage of UGS area (*PUGS)* and UGS area per inhabitant (*UPI)* - assess the quantity of green spaces in a neighbourhood. The three metrics- UGS patch density (*UPD),* Mean area of UGS patches (*Area_MN)* and Mean Euclidean distance between neighbouring green space patches (*ENN_MN)*- are associated with size and fragmentation of green space patches in a neighbourhood. Essentially these metrics describe the quality aspect of green space distribution since small, fragmented and distant patches signify poorer quality than large and contiguous patches (*Tian et al., 2014; Li and Liu, 2016; You, 2016*). The remaining two metrics- Area weighted mean fractal dimension index (*FRAC_AM*) and Aggregation index (*AI*)- are related to the shape complexity and aggregation of green space patches in a neighbourhood. Compared with simple-shaped and aggregated patches, complex-shaped and disaggregated patches increase the proximity between green spaces and residents (*Jim, 2013; Tian et al., 2014*). Hence, these two metrics reckon the level of accessibility to green spaces in a neighbourhood (*Sathyakumar et al., 2018*).

The spatial metrics of green spaces were computed for 2001 and 2011 from the respective green space maps using eight-cell neighbourhood criteria in Fragstats v4.2 (*McGarigal et al., 2012*). These metrics were assessed for each census section using the newly created shapefile, and the neighbourhood-level green space distribution indicators were derived for both years.

3.2.5 Spatiotemporal pattern analysis

The spatiotemporal variations in green space distribution were analysed in two stages. In the first stage, maps of green space distribution indicators in 2001 and 2011, and the change in indicator values between 2001 and 2011 were generated. These maps aid visual identification of spatiotemporal patterns of green space distribution among the census sections but do not reveal the hotspots of green space improvement/degradation (*Zhang et al., 2008*). Hence, in the second stage, Local Indicator of Spatial Autocorrelation (LISA) analyses were performed to reveal the statistically significant clusters and outliers. The LISA analyses were performed using local Moran's I (*Anselin, 1995*), a widely used statistic to identify statistically significant landscape patterns (*Bardhan et al., 2016; Mehrotra et al., 2018; Hughey et al., 2018*).

In this study, the local Moran's I (I_i) of each green space distribution indicator x for a census section i was computed as in Eq.1 (*Anselin, 1995*):

$$I_i = \frac{(x_i - \bar{X})}{\sigma^2} \sum_{j=1, j \neq i}^{n} w_{i,j}(x_j - \bar{X}) \qquad (1)$$

where x_i and x_j are the values of x in census sections i and j; $\bar{X}$ is the mean of x; σ^2 is the variance of x; n is the number of census sections; $w_{i,j}$ is the spatial weight assigned between census sections i and j.

Local Moran's I ranges between -1 and +1, wherein -1 signifies spatial outliers, +1 signifies spatial clusters, and 0 signifies random clustering. Here, spatial outliers refer to: i) census sections having high values of a green space distribution indicator surrounded by sections with low values (High-Low), or ii) census sections having low values of a green space distribution indicator surrounded by sections with high values (Low-High). Spatial clusters refer to census sections with high or low values of a green space distribution indicator surrounded by similar sections (High-High or Low-Low). The values of a distribution indicator in a census section is considered high or low with reference to the mean of that indicator (*GeoDa, 2019*). The significance of the computed local Moran's I is tested against the null hypothesis of no spatial autocorrelation to determine the statistically significant spatial clusters and outliers (*Hughey et al., 2018*).

For each green space distribution indicator, we generated the corresponding LISA maps depicting the neighbourhood clusters and outliers in both 2001 and 2011. A comparison of these two maps revealed the temporal changes in spatial patterns of that indicator during the study period. Further, for each indicator, we assessed the variation in values between 2001 and 2011 (i.e. value in 2011 minus value in 2001), and generated the corresponding LISA map. This map revealed the spatial clusters and outliers of temporal changes in that green space distribution indicator during the study period. The LISA analyses were performed in GeoDa 1.6.6 using first order queen contiguity-based spatial weights, and were tested with 999 permutations at 0.05 significance level.

Table 1
Description of urban green space distribution indictors used in the study.

Indicator	Formula	Description	Units and Range
Percentage of UGS area (*PUGS*)	$PUGS = \frac{A_{UGS}}{A_{CS}} * 100$	where A_{UGS} is the area (in m^2) of UGS in the census section, and A_{CS} is the area (in m^2) of the census section.	Percent; $0 \leq PUGS \leq 100$
UGS area per inhabitant (*UPI*)	$UPI = \frac{A_{UGS}}{P_{CS}}$	where A_{UGS} is the area (in m^2) of UGS in the census section, and P_{CS} is the population of the census section.	m^2 per person; $UPI \geq 0$
Urban green space patch density# (*UPD*)	$UPD = \frac{n}{A_{CS}} * 10^6$	where n is the number of UGS patches in the census section, and A_{CS} is the area (in m^2) of the census section.	number per km^2; $UPD \geq 0$
Mean area# of UGS patches (*Area_MN*)	$Area\_MN = \frac{A_{UGS}}{n} * 10^{-4}$	where A_{UGS} is the area of UGS (in m^2) in the census section, n is the number of UGS patches in the census section.	ha; $Area\_MN \geq 0$
Mean Euclidean nearest neighbour distance# of UGS patches (*ENN_MN*)	$ENN\_MN = \frac{\sum_{i=1}^{n} d_i}{n}$	where d_i is the distance (in m) between an UGS patch i and its nearest neighbouring patch in the census section, n is the number of UGS patches in the census section.	m; $ENN\_MN > 0$
Area weighted mean fractal dimension index# of UGS patches (*FRAC_AM*)	$FRAC\_AM = \sum_{i=1}^{i=n} \left[\left(\frac{a_i}{A_{UGS}} \right) \left(\frac{2 \ln 0.25\, p_i}{\ln a_i} \right) \right]$	where a_i and p_i denote the area (in m^2) and perimeter (in m) of an UGS patch i respectively, n is the number of UGS patches in the census section, A_{UGS} is the area (in m^2) of UGS in the census section.	Unitless; $1 \leq FRAC\_AM \leq 2$ $FRAC\_AM = 1$ if the patches are square-shaped. $FRAC\_AM = 2$ if the patches are highly convoluted.
Aggregation index# of UGS patches (*AI*)	$AI = \left[\frac{J}{\max J} \right] * 100$	where J is the number of joins between pixels of UGS patches in the census section based on single-count method, *max J* is the maximum possible value of J.	Percent; $0 \leq AI \leq 100$ AI = 0 if the patches are maximally disaggregated. AI = 100 if the patches are maximally compact.

#Source: *McGarigal (2015)*.
Adapted from *Sathyakumar et al. (2018)*.

4. Results

The first part of this section presents the green space maps of Mumbai in 2001 and 2011 and their estimated accuracies. The second part deals with changes in city level urban green space distribution indicators between 2001 and 2011. The third part analyses the spatiotemporal patterns of neighbourhood (i.e. census section) level green space distribution indicators during the same period.

4.1 Urban green space maps and their accuracies

The maps of urban green spaces in Mumbai in the years 2001 and 2011 are presented in Fig. 3 and Fig.4 respectively. The prominent green spaces in these maps include the Sanjay Gandhi National Park in the north, mangroves in the northwest and east, a few hills in the eastern suburbs, and the race course area in the south.

The error matrices generated for the green space maps of 2001 and 2011 are given in Table 2 and Table 3 respectively. The cell entries in these tables represent the percentage of area in their respective maps. From Table 2, it is observed that the estimated overall accuracy of the green space map of 2001 is 88.03% (58.53%+29.50%). The standard error of this overall accuracy was estimated to be 1.66%, which yields a 95% confidence interval of 84.78% to 91.28%. Similarly, from Table 3, it is observed that the estimated overall accuracy of the green space map of 2011 is 83.11% (44.00%+39.11%). The standard error of this overall accuracy was estimated to be 1.88%, which yields a 95% confidence interval of 79.42% to 86.78%. The conventional error matrices based on sample count are presented in Appendix A.

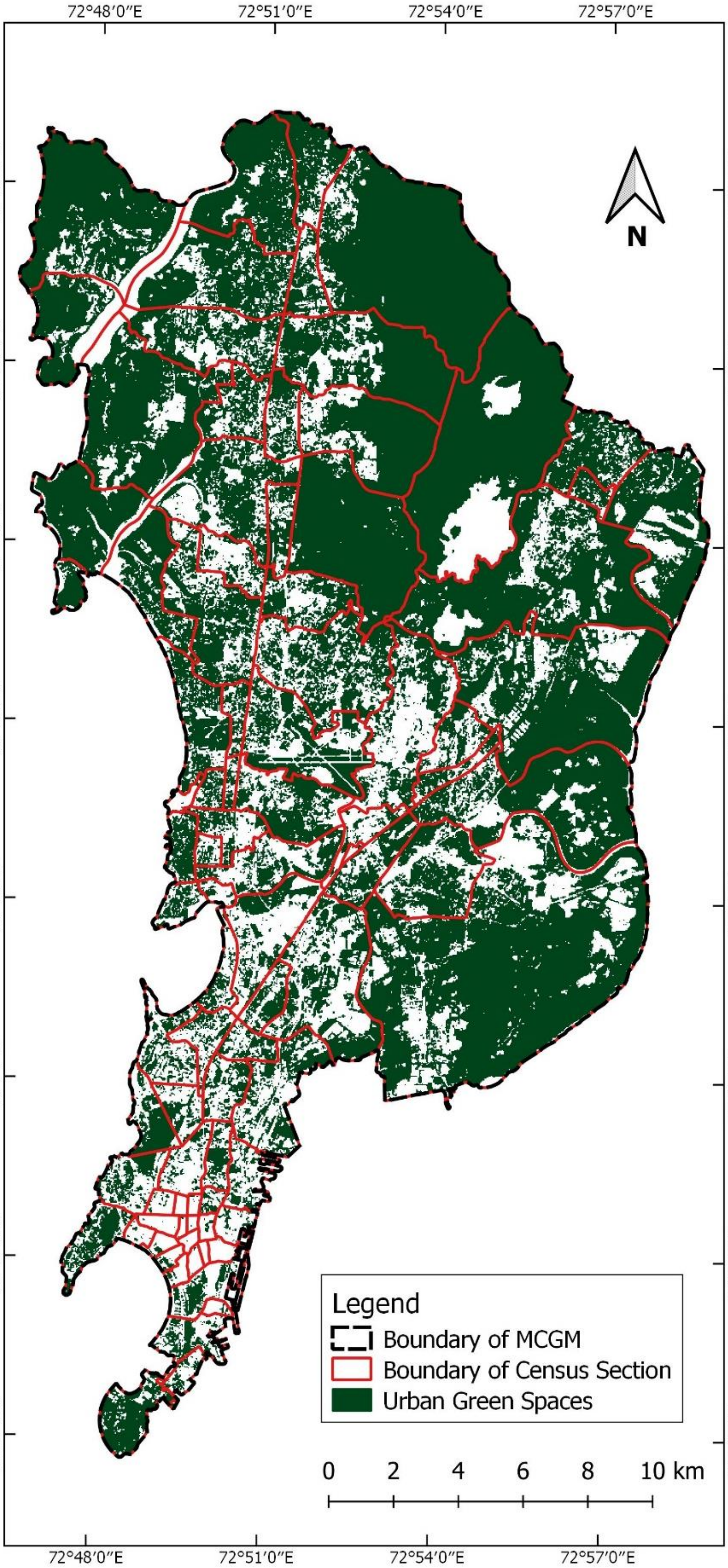

349 **Fig. 3.** Map of urban green spaces in Mumbai in 2001.

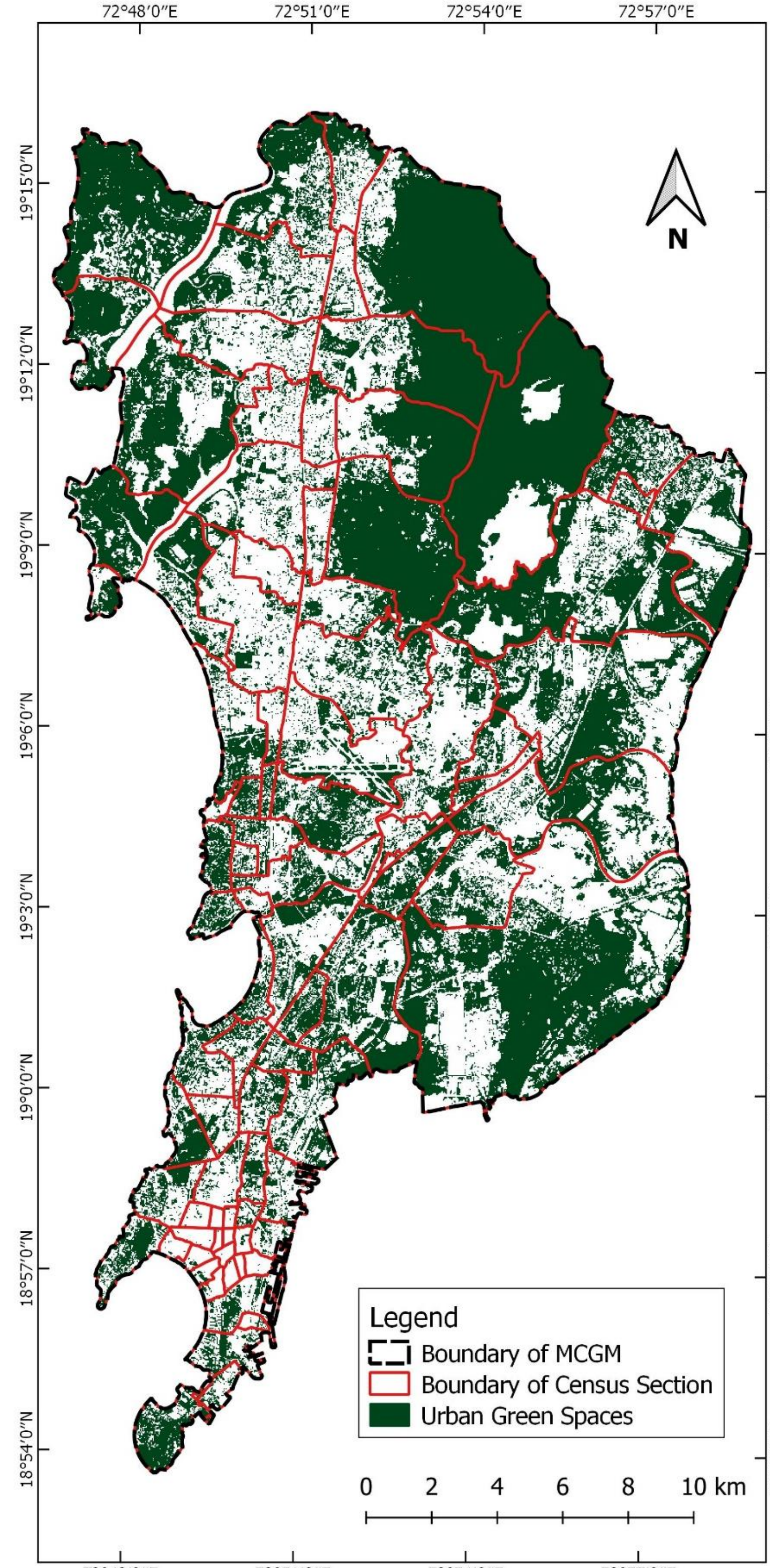

350 **Fig. 4.** Map of urban green spaces in Mumbai in 2011.

Table 2
Error matrix of the urban green spaces (UGS) map of Mumbai in 2001.

Map	Reference		Total	User's Accuracy (Std. Error)	n
	UGS	Non-UGS			
UGS	58.53 %	8.72 %	67.25 %	87.03 % (2.18%)	239
Non-UGS	3.25 %	29.50 %	32.75 %	90.01 % (2.36%)	161
Total (Std. Error)	61.78 % (1.65%)	38.22 % (1.65%)	100%		400
Producer's Accuracy (Std. Error)	94.73 % (1.19%)	77.17 % (2.99%)			
n	224	176	400		

Adapted from *Stehman and Foody (2019).*

Table 3
Error matrix of the urban green spaces (UGS) map of Mumbai in 2011.

Map	Reference		Total	User's Accuracy (Std. Error)	n
	UGS	Non-UGS			
UGS	44.00 %	8.05 %	52.05 %	84.54 % (2.60%)	194
Non-UGS	8.84 %	39.11 %	47.95 %	81.55 % (2.71%)	206
Total (Std. Error)	52.84 % (1.87%)	47.16 % (1.87%)	100%		400
Producer's Accuracy (Std. Error)	83.26 % (2.09%)	82.92 % (2.43%)			
n	202	198	400		

Adapted from *Stehman and Foody (2019).*

4.2 Temporal changes in city level urban green space distribution

A comparison of the two green space maps (Figs. 3 and 4) revealed that between 2001 and 2011 much of Mumbai's urban green spaces had disappeared, especially in the western suburbs. Also, some neighbourhoods in the southern part of City District were found to lack green cover in both the years. Further, to quantitatively assess the temporal changes in Mumbai's green cover, the green space distribution indicators derived for the years 2001 and 2011 are listed in Table 4.

Table 4

Temporal changes in city level urban green space distribution indicators.

Year	Population	UGS area (km^2)	UGS distribution indicators						
			***PUGS* (%)**	***UPI* (m^2 per person)**	***UPD* (per km^2)**	***Area_MN* (ha)**	***ENN_MN* (m)**	***FRAC_AM***	***AI* (%)**
2001	11,978,450	317.74	67.29	26.52	3.50	19.19	75.16	1.32	91.35
2011	12,442,373	245.92	52.08	19.76	10.38	5.01	71.75	1.31	85.16

The results provided in Table 4 show that Mumbai lost 22.6% of its urban green spaces between 2001 and 2011. Subsequently, the percentage of green space area (*PUGS*) in the city reduced by 15.21 percentage points during this period. Further, the decrease in green spaces, accompanied by population increase, eventually led to a fall in green space area per capita (*UPI*) by 6.76 m^2. Also, in this period, the green spaces became more fragmented as evident from the threefold increase in green space patch density (*UPD*) values. Further, the study period saw the average green space patch (*Area_MN*) in Mumbai shrink by almost four times. In the context of the above findings, the decrease in nearest neighbour distance (*ENN_MN*) between green space patches could be attributed to the disintegration of larger patches and the disappearance of distant patches. Concerning shape complexity, the similarity observed in *FRAC_AM* values was potentially due to obscurity of fine changes in patch shapes at the spatial resolution used (30m). Finally, the aggregation index (*AI*) values suggest that green spaces relatively disaggregated during the study period. Thus, the green spaces in Mumbai overall turned smaller, fragmented and disaggregated during 2001-11.

4.3 Spatiotemporal patterns of neighbourhood level urban green space distribution indicators

Table 5 lists the descriptive statistics of the seven green space distribution indicators derived at neighbourhood (i.e. census section) level for the years 2001 and 2011. Table 5 as well as Figs. 3 and 4 show that the census sections 7 and 10 turned greenless by 2001 and 2011 respectively. Further findings related to spatiotemporal patterns of each indicator at census section level are presented in the following sub-sections.

Table 5
Descriptive statistics of neighbourhood level urban green space distribution indicators assessed for the years 2001 and 2011.

Indicator	Year	Median	Minimum		Maximum	
			Value	Location[#]	Value	Location[#]
PUGS *(%)*	2001	50.02	0	CS 7	96.62	CS 59
	2011	38.96	0	CS 7,10	88.86	CS 59
UPI *(m^2 per person)*	2001	12.42	0	CS 7	2501.41	CS 71
	2011	9.62	0	CS 7,10	1873.81	CS 71
UPD *(per km^2)*	2001	7.93	0	CS 7	35.09	CS 76
	2011	15.88	0	CS 7,10	40.93	CS 76
Area_MN *(ha)*	2001	5.14	0	CS 7	228.07	CS 59
	2011	1.93	0	CS 7,10	71.83	CS 61
*ENN_MN** *(m)*	2001[**]	73.62	60	CS 41,66	722.49	CS 13
	2011[***]	71.66	61.77	CS 24	238.71	CS 13
FRAC_AM	2001[$]	1.20	1	CS 12,26	1.30	CS 52
	2011[$$]	1.19	1	CS 12,26	1.31	CS 87
AI *(%)*	2001[†]	81.82	0	CS 26	100	CS 10
	2011[††]	71.66	14.29	CS 6	100	CS 11

[#]CS stands for census section.
*The minimum *ENN_MN* is twice the pixel size when 8-cell neighbourhood criteria is used (*McGarigal, 2015*). Hence, in this study, the minimum possible *ENN_MN* is 60m.
[*]Census sections 7, 10 and 12 were ignored as they had fewer than two green space patches.
[**]Census sections 7, 10, 11, 12 and 26 were ignored as they had fewer than two green space patches.
[$]Census section 7 was ignored as it had no green cover.
[$$]Census sections 7 and 10 were ignored as they had no green cover.
[†]Census sections 7 and 12 were ignored as they had fewer than two green space pixels.
[††]Census sections 7, 10, 12 and 26 were ignored as they had fewer than two green space pixels.

4.3.1 *Percentage of urban green space area (PUGS)*

The *PUGS* of census sections ranged from 0 to 96.62% in 2001 and from 0 to 88.86% in 2011 (Table 5). The *PUGS* maps of census sections in 2001 and 2011 (Fig. 5a and Fig. 5b) reveal that census sections mostly witnessed decrease in *PUGS* during the period. This is also evident from the decrease in median *PUGS* by 11 percentage points between 2001 and 2011

(Table 5). The change in *PUGS* during the study period was in the range of -45.01 percentage points (census section 58) to +10.00 percentage points (census section 31). The map of change in *PUGS* (Fig. 5c) shows that sixty eight census sections, mostly in the suburbs, saw a decrease in *PUGS*. These findings indicate the gradual disappearance of green cover in large parts of Mumbai, especially in the suburbs.

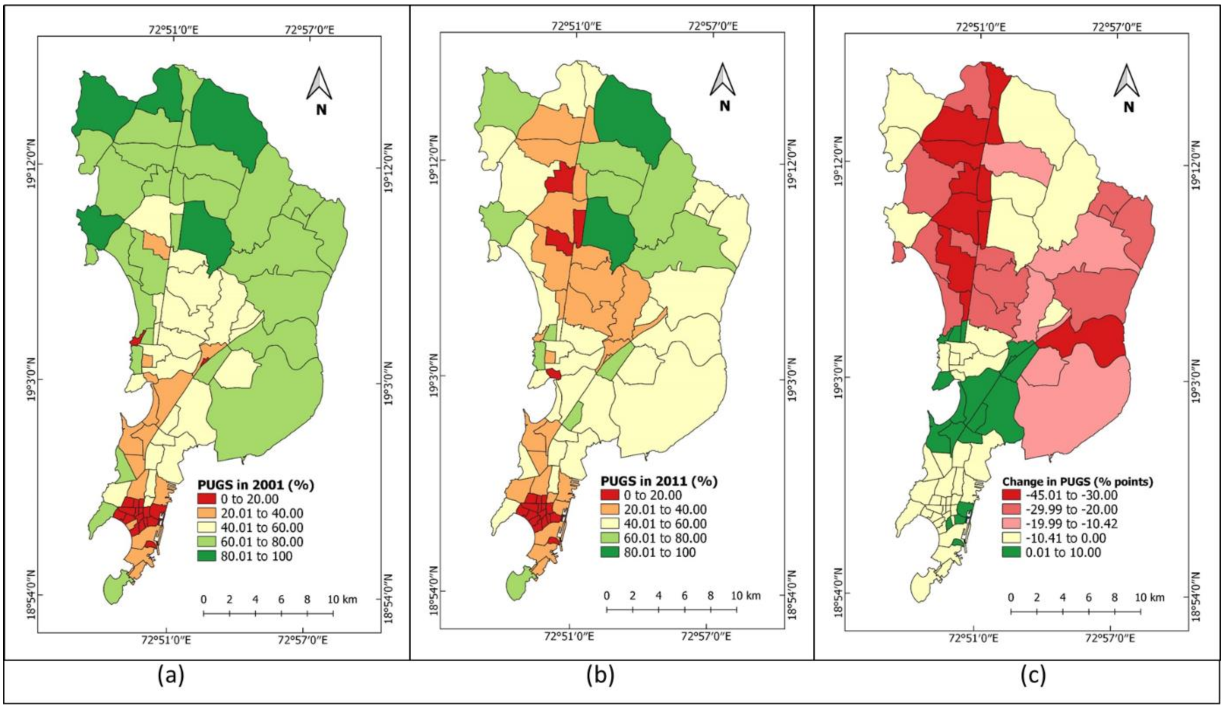

Fig. 5. Map of (a) *PUGS* in 2001, (b) *PUGS* in 2011, and (c) change in *PUGS* during 2001-11.

The LISA maps[1] of *PUGS* in the years 2001 and 2011 (Fig. 6a and Fig. 6b) present the statistically significant clusters and outliers. These maps identify the individual census sections that constituted the high *PUGS* clusters (dark red) in the suburbs and the low *PUGS* clusters (dark blue) in the City District. Additionally, these maps highlight the outlier census sections in both years. For example, in 2011 (Fig. 6b), the sections numbered 72 and 78 (light blue) had

[1] Interpretation of LISA maps is illustrated using the example of Fig. 6a. The mean *PUGS* of census sections in 2001 was 47.19%. Based on this mean value and the significance level of local Moran's I for each section, the spatial clusters (High-High and Low-Low) and outliers (High-Low and Low-High) were identified. The 'High-High' sections (dark red) and their neighbours have significantly high values of *PUGS*. The 'Low-Low' sections (dark blue) and their neighbours have significantly low values of *PUGS*. The 'Low-High' sections (light blue) indicates the sections with significantly low *PUGS* that are surrounded by sections with high *PUGS*. The 'High-Low' sections (light red) indicates the sections with significantly high *PUGS* that are surrounded by sections with low *PUGS* (*GeoDa, 2019*).

significantly low *PUGS* than their neighbours, and thus deserve special attention. On the other hand, the section numbered 20 (light red) had high *PUGS* compared to its neighbours. Further, by comparing the two LISA maps (Fig. 6a and Fig. 6b), the specific census sections in the suburbs that lost their status as high *PUGS* hotpots could also be identified.

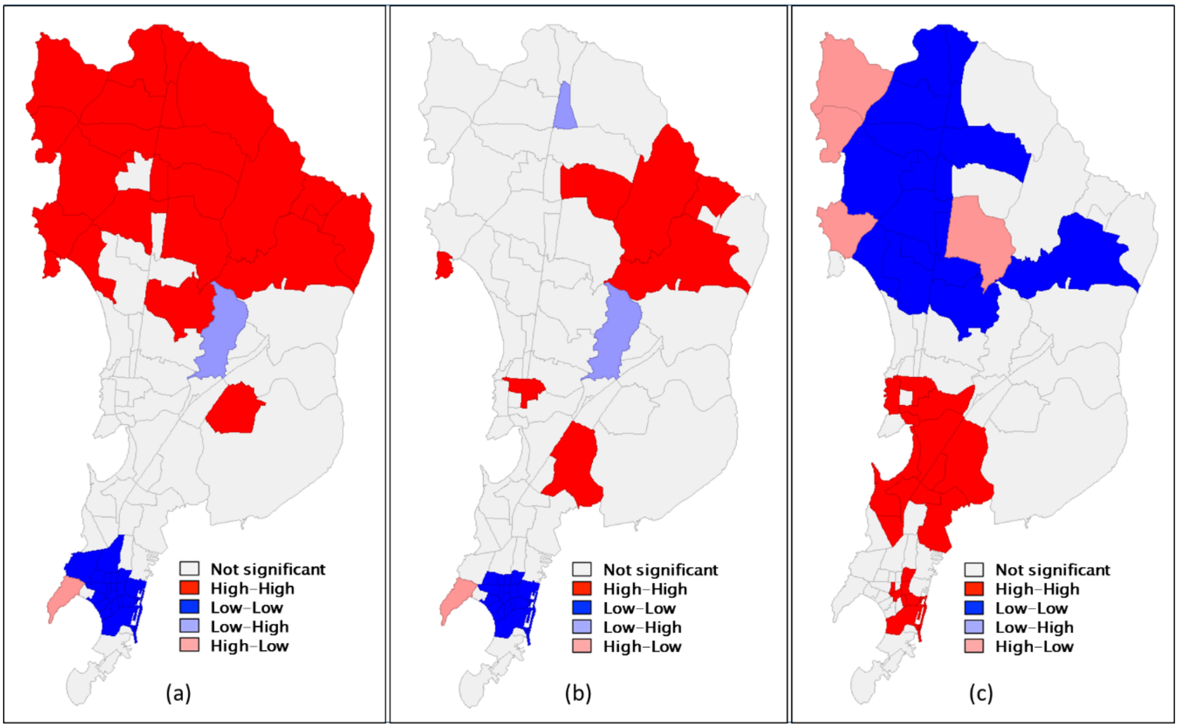

Fig. 6. LISA maps of (a) *PUGS* in 2001, (b) *PUGS* in 2011, and (c) change in *PUGS* during 2001-11.

The mean change in *PUGS* of all census sections during 2001-11 was -10.42 percentage points. Relative to this mean, the LISA map of change in *PUGS* (Fig. 6c) depicts the census sections as 'high' (values from -10.42 to +10.00) and 'low' (values from -45.01 to -10.42). This map distinguishes the particular sections that witnessed severe reduction in *PUGS* (dark blue) as well as improvement in *PUGS* (dark red). This map also confirms that the un-greening phenomenon was more acute in the northern part of western suburbs, while the improvement in *PUGS* was focussed mainly in the City District.

4.3.2 *Urban green space area per inhabitant (UPI)*

The *UPI* of census sections ranged from 0 to 2501.41 m^2 per person in 2001 and 0 to 1873.81 m^2 per person in 2011 (Table 5). The *UPI* maps of census sections in 2001 and 2011 (Fig. 7a and Fig. 7b) reveal that in both years most sections in the City District had lower *UPI*. Further, it is observed that many sections in the western suburbs saw a decrease in *UPI* during 2001-11.

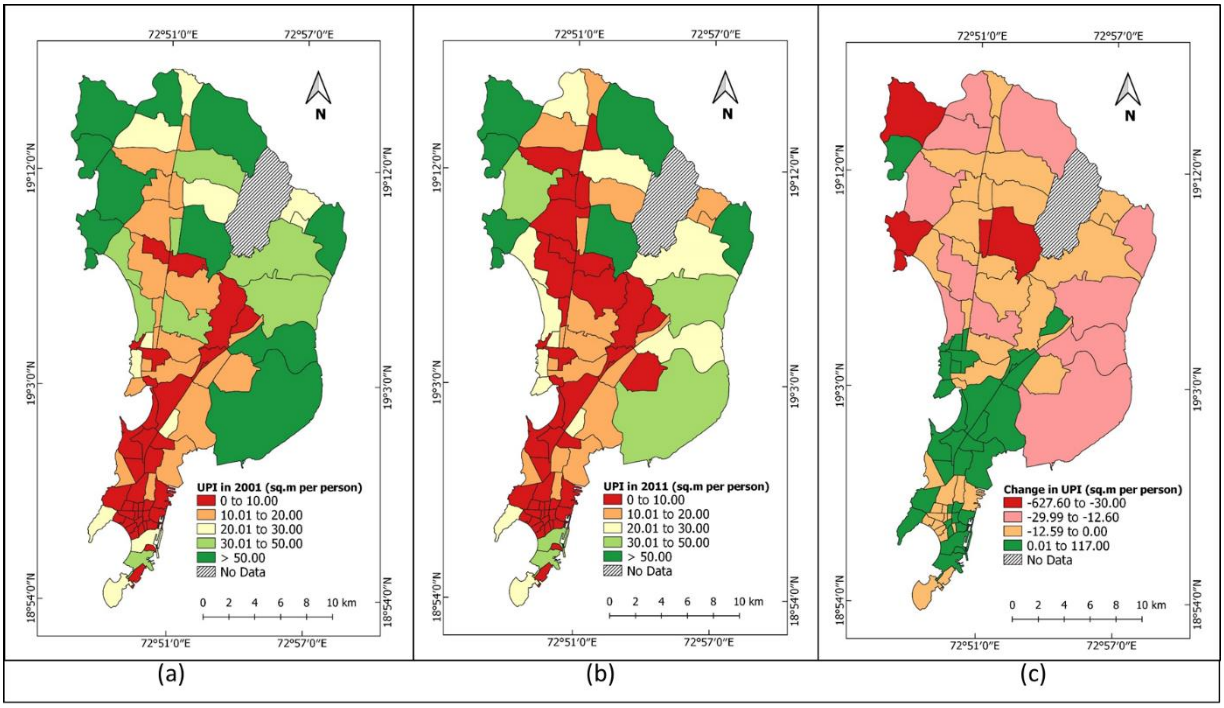

Fig. 7. Map of (a) *UPI* in 2001, (b) *UPI* in 2011, and (c) change in *UPI* during 2001-11.

The median *UPI* decreased by 2.8 m^2 per person between 2001 and 2011 (Table 5). The change in *UPI* between 2001 and 2011 was in the range of -627.60 m^2 per person (census section 71) to +117.00 m^2 per person (census section 66). The map of change in *UPI* (Fig. 7c) reveals that fifty three census sections witnessed a decrease in *UPI* while thirty four saw an increase. The remaining census section numbered 7 had no green cover in both the years. However, as *UPI* is impacted not only by changing green space area but also by changing population, a case-by-case analysis was performed to identify the principal cause driving the change in *UPI* during 2001-11. The analysis results given in Table 4 reveal that i) rise in *UPI* was mainly due to decreasing population (30 out of 34 cases), and ii) decline in *UPI* was mainly due to the decrease in urban green space area (all 53 cases). Also, only four census sections (numbered 32, 33, 40 and 42) were found to have a healthy increase in green space area vis-à-vis rising population. Similarly, twenty three census sections saw a decrease in green space area despite their dwindling population.

Table 4
Primary cause of change in *UPI* of census sections during 2001-11.

Change in *UPI*	**Number of cases**	**Change in UGS area**	**Change in Population**		**Total**
			Positive	Negative	
Positive	34	Positive	4	14	**18**
		Zero	0	1	**1**
		Negative	0	15	**15**
		Total	**4**	**30**	34
Negative	53	Positive	0	0	**0**
		Negative	30	23	**53**
		Total	**30**	**23**	53

The LISA maps of *UPI* in the years 2001 and 2011 (Fig. 8a and Fig. 8b) present the statistically significant clusters and outliers. These maps show that the mangrove-rich coastal census sections 54, 66 and 71 formed the clusters of high *UPI* (dark red) while the southern part of City District housed the low *UPI* clusters (dark blue) in both years. Further, as shown in Fig.8b, the three census sections numbered 67, 69 and 70 (light blue) had significantly low *UPI* than their neighbours in 2011, and thus require more attention.

The mean change in *UPI* of all census sections was -12.60 m^2 per person. Relative to this mean, the LISA map of change in *UPI* (Fig. 8c) portrays the census sections as ‘high’ (values from -12.60 to +117.00) and ‘low’ (values from -627.60 to -12.60). The map shows that the decline in *UPI* was severe in and around the census sections 54 and 70 (dark blue) in western suburbs. On the other hand, the sections 4, 6 and 13 (dark red) and their neighbours in the City District experienced improvement in *UPI*. This improved *UPI* was a result of decrease in population levels caused by gentrification in these sections (*Pethe et al., 2014*). Further, the map indicates that the census section 71 (light blue) requires additional focus, as it experienced significantly steep decline in *UPI* than its neighbours (Fig. 8c), though it still had significantly high *UPI* in 2011 (Fig. 8b, Table 5).

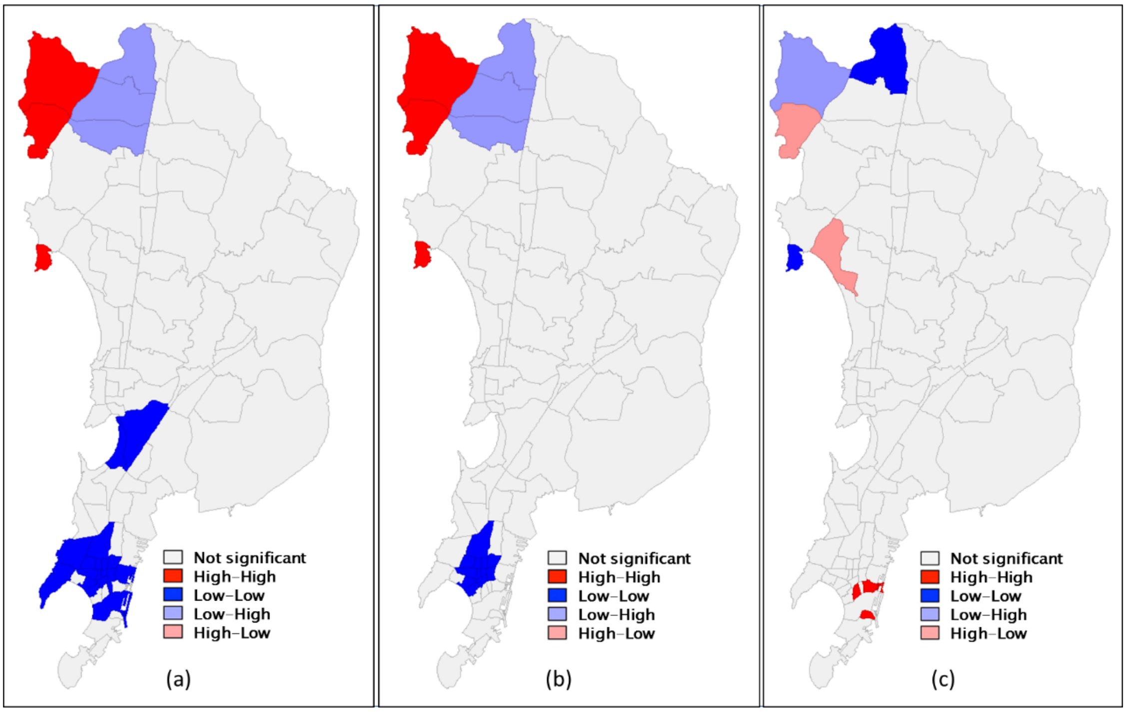

Fig. 8. LISA maps of (a) *UPI* in 2001, (b) *UPI* in 2011, and (c) change in *UPI* during 2001-11.

4.3.3 *Urban green space patch density (UPD)*

The *UPD* of census sections ranged from 0 to 35.09 patches per km^2 in 2001 and from 0 to 40.93 patches per km^2 in 2011 (Table 5). The *UPD* maps of census sections in 2001 and 2011 (Fig. 9a and Fig. 9b) show that several sections across Mumbai witnessed increase in *UPD* between 2001 and 2011. This is confirmed by the rise in median *UPD* by 7.95 patches per km^2 between these years (Table 5). The change in *UPD* during the study period was in the range of -14.20 patches per km^2 (census section 47) to +33.60 patches per km^2 (census section 62). The map of change in *UPD* (Fig. 9c) reveals that seventy three sections witnessed an increase in *UPD* values. Since *UPD* could be altered even due to addition of new green space patches, we analysed the level of increase in *PUGS* in these seventy three sections. It was observed that sixty two sections had lost green space area while the remaining eleven had gained. This suggests that increase in *UPD* was predominantly due to fragmentation rather than augmentation of green cover.

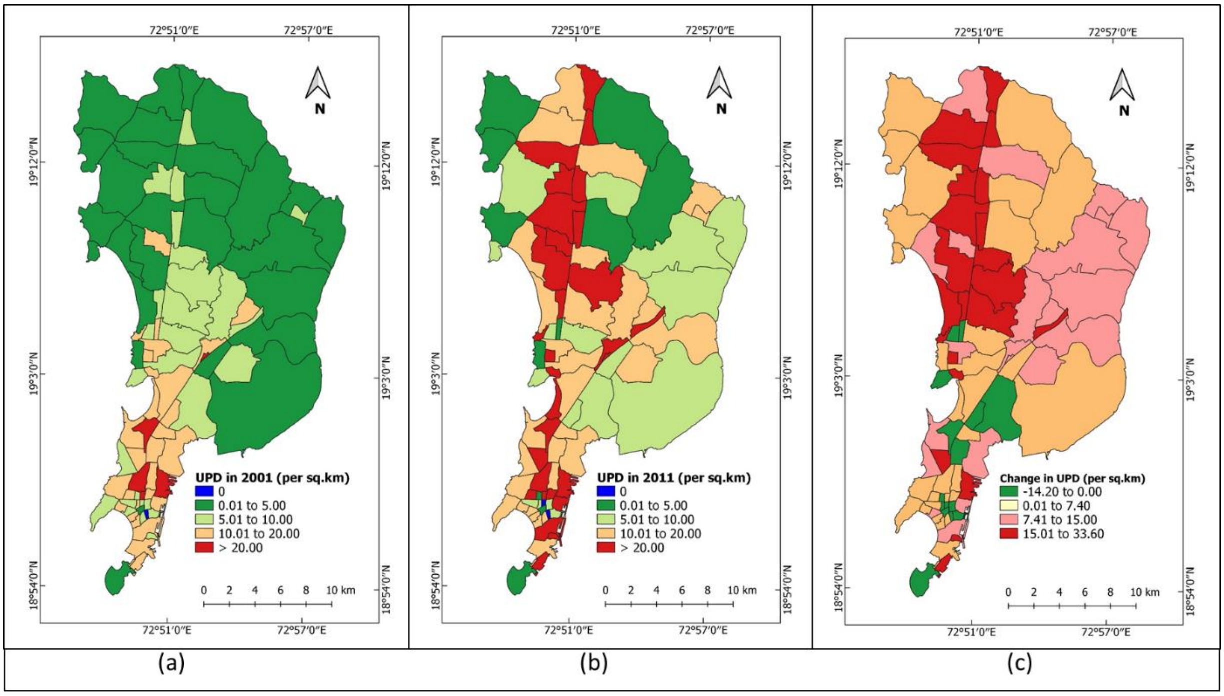

Fig. 9. Map of (a) *UPD* in 2001, (b) *UPD* in 2011, and (c) change in *UPD* during 2001-11.

The LISA maps of *UPD* in the years 2001 and 2011 (Fig. 10a and Fig. 10b) present the statistically significant clusters and outliers. These maps show that, in 2001, the northern part of the suburbs largely formed clusters of low *UPD* (dark blue) while the central part of City District constituted the clusters of high *UPD* (dark red). However, by 2011 the extent of low *UPD* clusters (dark blue) in the suburbs decreased considerably and the high *UPD* clusters (dark red) shifted from City District to the western suburbs. These results indicate extensive disintegration of previously continuous green space patches in the western suburbs.

The mean change in *UPD* of all census sections was +7.40 patches per km^2. Relative to this mean, the LISA map of change in *UPI* (Fig. 10c) characterises the census sections as 'high' (values from +7.40 to +33.60) and 'low' (values from -14.20 to +7.40). This map shows that the spurt in *UPD* was focussed in northern part of the western suburbs (dark red), while the decrease in *UPD* was concentrated in the City District (dark blue). Thus, it is confirmed that the western suburbs encountered intense fragmentation of green spaces during 2001-11

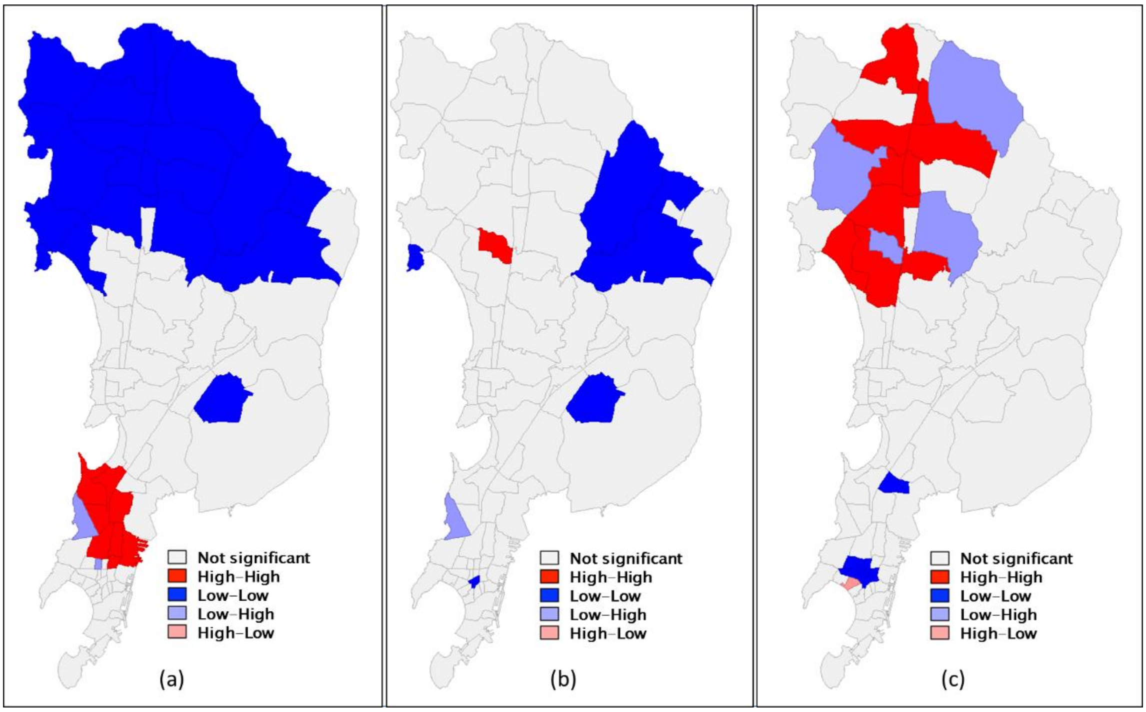

Fig. 10. LISA maps of (a) *UPD* in 2001, (b) *UPD* in 2011, and (c) change in *UPD* during 2001-11.

4.3.4 *Mean area of urban green space patches (Area_MN)*

The *Area_MN* of census sections ranged from 0 to 228.07 ha in 2001 and from 0 to 71.83 ha in 2011 (Table 5). The *Area_MN* maps of census sections in 2001 and 2011 (Fig. 11a and Fig. 11b) reveal that large parts of Mumbai saw decrease in *Area_MN* during this period. This trend is also reflected in the decrease in median *Area_MN* by 3.21 ha between these years (Table 5). The change in *Area_MN* during the study period was in the range of -177.74 ha (census section 59) to +9.36 ha (census section 47). The map of change in *Area_MN* (Fig. 11c) reveals that seventy four census sections saw a decrease in *Area_MN* during 2001-11. This shrinkage in *Area_MN* is symptomatic of the diminution and disintegration of green spaces in most parts of Mumbai during the study period.

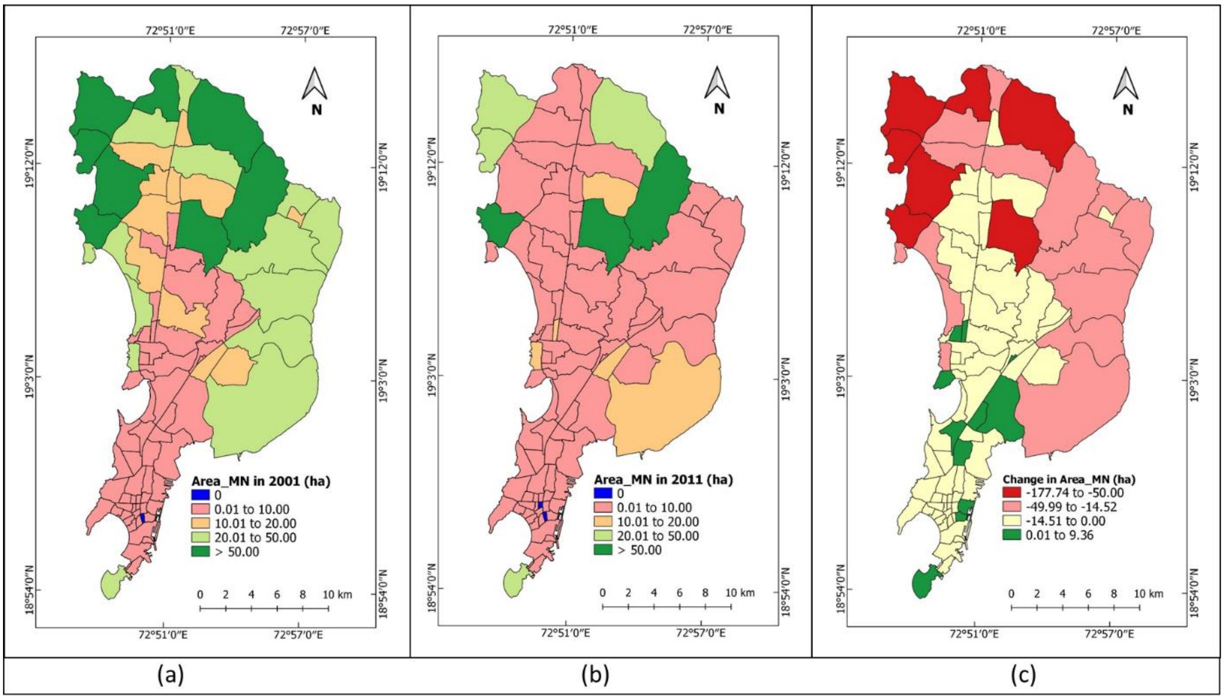

Fig. 11. Map of (a) *Area_MN* in 2001, (b) *Area_MN* in 2011, and (c) change in *Area_MN* during 2001-11.

The LISA maps of *Area_MN* in the years 2001 and 2011 (Fig. 12a and Fig. 12b) present the statistically significant clusters and outliers. In both years, the high *Area_MN* clusters (dark red) were found in the suburbs while the clusters of low *Area_MN* (dark blue) were located mainly in City District. Further, it was noticed that extents of both high *Area_MN* clusters (dark red) in the suburbs and low *Area_MN* clusters (dark blue) in City District shrank by 2011. This was due to the intense reduction in *Area_MN* in the western suburbs to levels similar to that of City District. For example, *Area_MN* of the census section 52 (the western suburb shown in dark blue in Fig. 12b) reduced by 12.04 ha from 12.84 ha in 2001 to 0.80 ha in 2011. This reduction is much higher than the maximum reduction in *Area_MN* experienced by any section in City District (census section 20; -3.76 ha). Also, the Fig. 12b signifies that adequate attention must be paid to census sections 54, 68 and 87 (light blue), which had significantly low *Area_MN* than their neighbours.

The mean change in *Area_MN* of all census sections was -14.52 ha. Relative to this mean, the LISA map of change in *Area_MN* (Fig. 12c) illustrates the census sections as 'high' (values from -14.52 to +9.36) and 'low' (values from -177.74 to -14.52). The map identifies the sections that saw drastic reduction in *Area_MN* during 2001-11 as well as those that saw minimal decrease or increase in *Area_MN*. This map also confirms that the decrease in *Area_MN* was more pronounced in certain suburban census sections (dark blue).

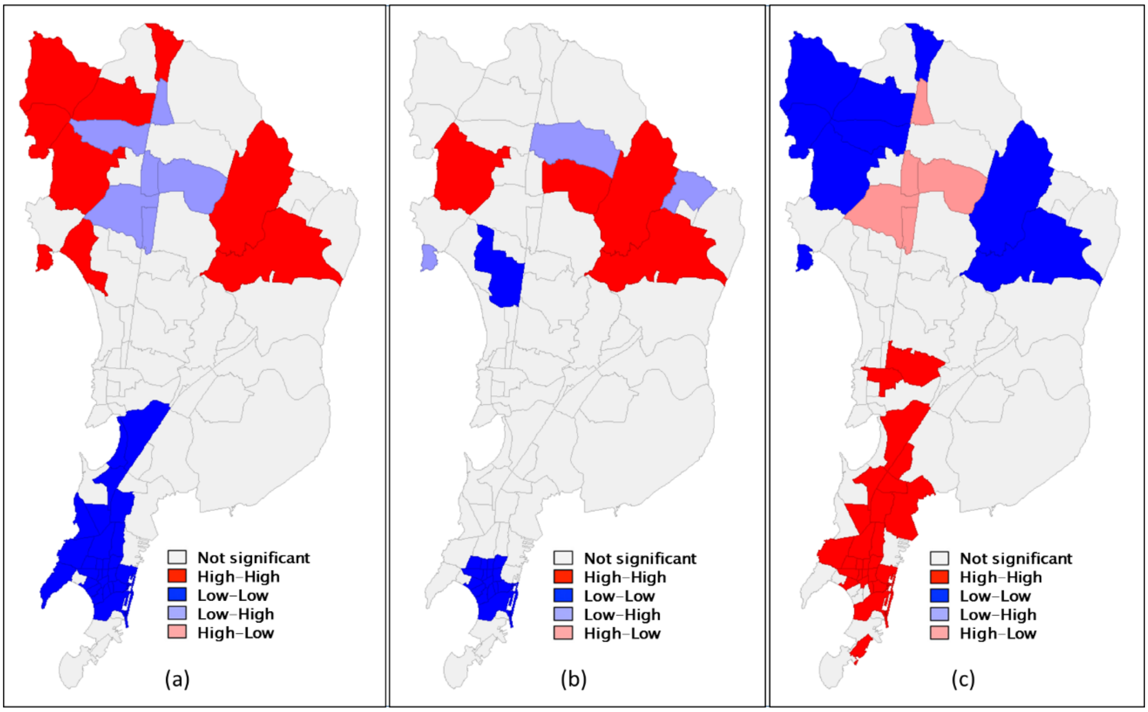

Fig. 12. LISA maps of (a) *AREA_MN* in 2001, (b) *AREA_MN* in 2011, and (c) change in *AREA_MN* during 2001-11.

4.3.5 *Mean Euclidean nearest neighbour distance of urban green space patches (ENN_MN)*

The *ENN_MN* of census sections ranged from 60 to 722.49 m in 2001 and from 61.77 to 238.71 m in 2011 (Table 5). The *ENN_MN* maps of census sections in 2001 and 2011 (Fig. 13a and Fig. 13b) reveal that most census sections had lower *ENN_MN* in both 2001 and 2011. The median *ENN_MN* was observed to have decreased by 1.96 m between 2001 and 2011 (Table 5). The change in *ENN_MN* during the study period was in the range of -483.78 m (census section 13) to +28.90 m (census section 18). The map of change in *ENN_MN* (Fig. 13c) reveals that fifty four census sections saw a decrease in *ENN_MN* whereas twenty nine sections saw an increase. The overall trend of decreasing *ENN_MN* was observed to be due to both rampant fragmentation and extinction of remote patches. Yet the change in *ENN_MN* of a census section was found to ultimately depend on whether the remnants of pre-existent patches lied near the core or on fringes.

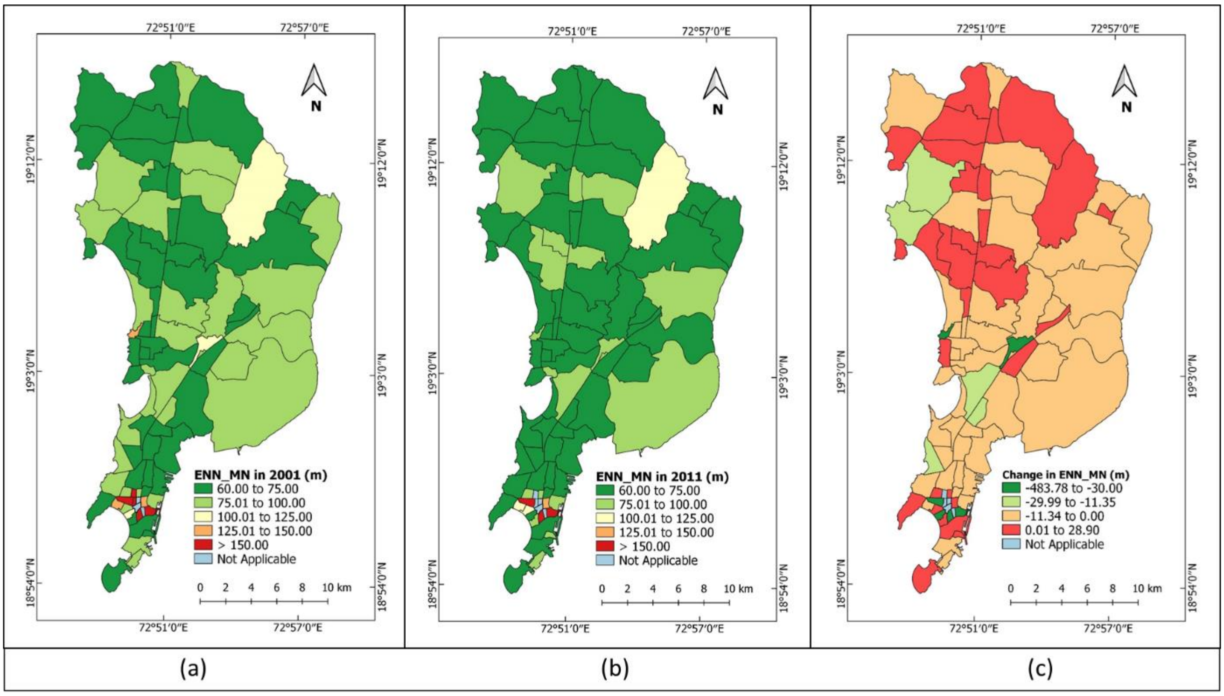

Fig. 13. Map of (a) *ENN_MN* in 2001, (b) *ENN_MN* in 2011, and (c) change in *ENN_MN* during 2001-11.

Note: The census sections with fewer than two green space patches are shown as 'Not Applicable' in these maps (refer footnotes under Table 5).

The LISA maps of *ENN_MN* in the years 2001 and 2011 (Fig. 14a and Fig. 14b) present the statistically significant clusters and outliers. In both years, a few adjacent census sections having sparse green cover in the southern part of City District (dark red) had *ENN_MN* much higher than the mean value of the respective years. For example, in 2001, the census sections 11, 13 and 26 had *ENN_MN* above 500 m against the mean of 101.42 m. Similarly, in 2011, the census sections 6, 8, 13, 16 had *ENN_MN* above 140 m against the mean of 78.59 m. The concentration of such high *ENN_MN* sections in these region in both years resulted in the observed clustering patterns.

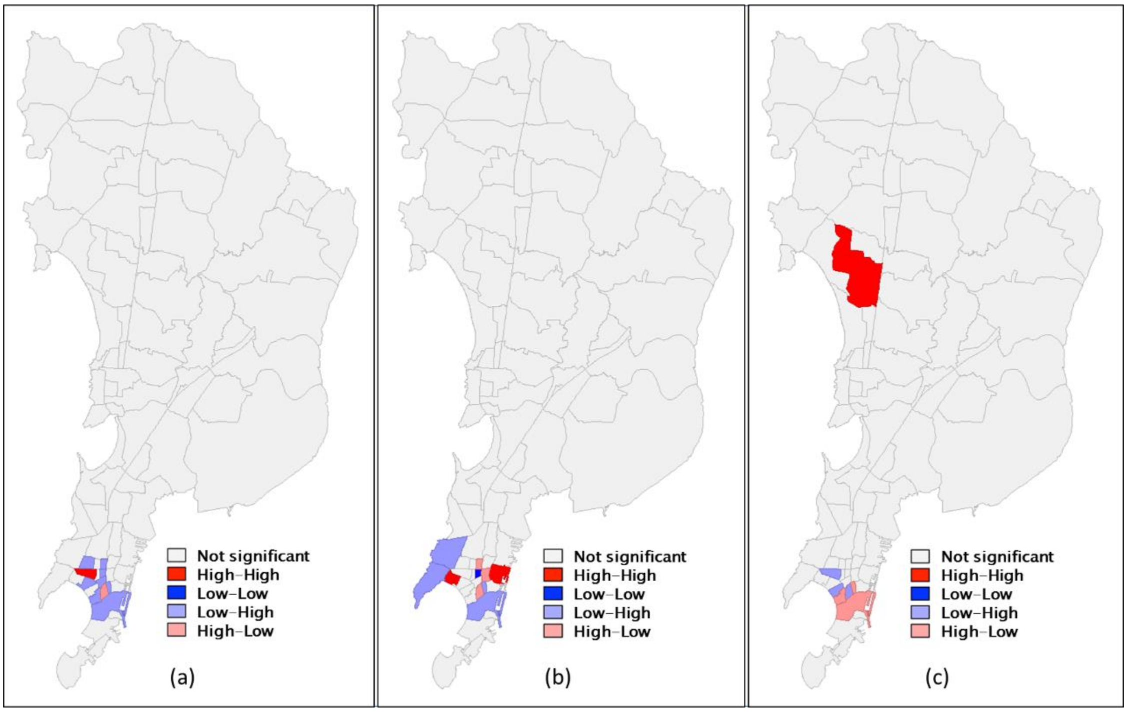

Fig. 14. LISA maps of (a) *ENN_MN* in 2001, (b) *ENN_MN* in 2011, and (c) change in *ENN_MN* during 2001-11.

The mean change in *ENN_MN* of all census sections was -11.35 m. Relative to this mean, the LISA map of change in *ENN_MN* (Fig. 14c) represents the census sections as 'high' (values from -11.35 to +28.90) and 'low' (values from -483.78 to -11.35). The map identifies the section 52 (dark red) and its neighbours as having experienced significantly high increase in *ENN_MN*. The southern part of City District exhibited a combination of 'high-low' and 'low-high' outliers (light red and light blue) indicating that the change in *ENN_MN* here was mixed.

4.3.6 *Area weighted mean fractal dimension index of urban green space patches (FRAC_AM)*

The *FRAC_AM* of census sections ranged from 1 to 1.30 in 2001 and 1 to 1.31 in 2011 (Table 5). The *FRAC_AM* maps of census sections in 2001 and 2011 (Fig. 15a and Fig. 15b) reveal that in both years the sections in southern part of City District had lower *FRAC_AM*, while most of the suburban sections had higher *FRAC_AM*. The median *FRAC_AM* was observed to have decreased marginally by 0.01 during 2001-11 (Table 5). Further, the change in *FRAC_AM* between 2001 and 2011 was in the range of -0.17 (census section 52) to +0.13

(census section 31). The map of change in *FRAC_AM* (Fig. 15c) reveals that fifty one census sections saw an increase in *FRAC_AM* whereas thirty four sections saw a decrease. These results suggest that green spaces in most census sections turned relatively complex-shaped between 2001 and 2011.

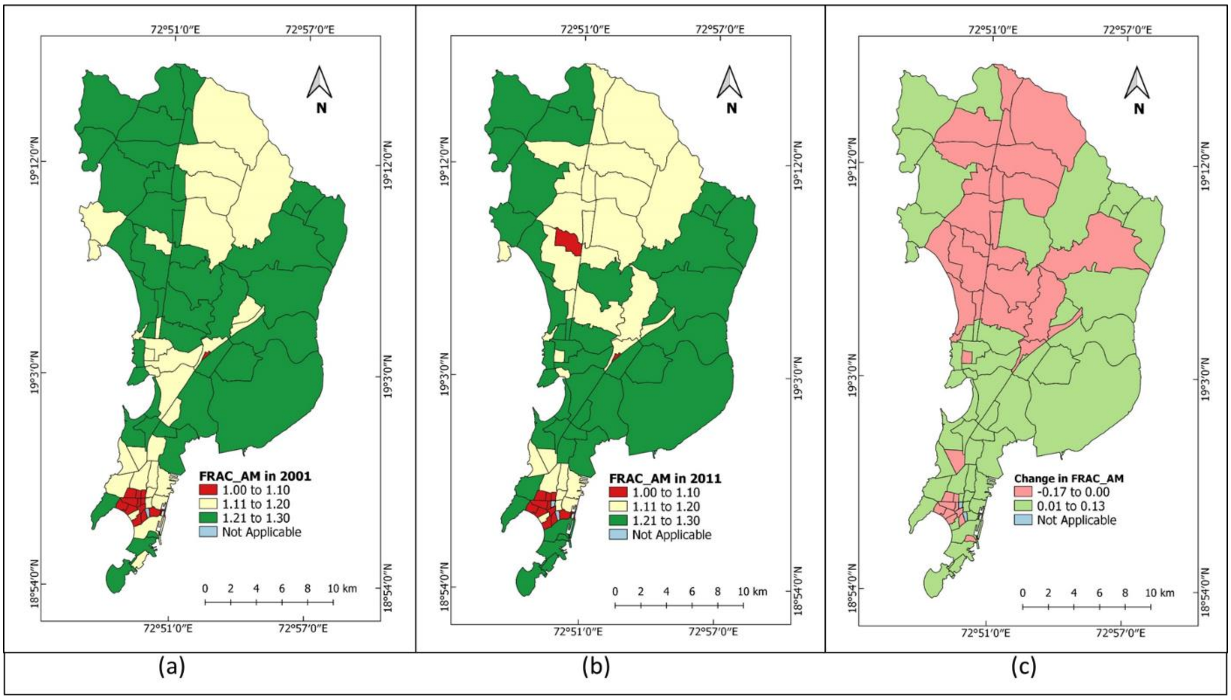

Fig. 15. Map of (a) *FRAC_AM* in 2001, (b) *FRAC_AM* in 2011, and (c) change in *FRAC_AM* during 2001-11.
Note: The census sections with no green cover are shown as 'Not Applicable' in the maps (refer footnotes under Table 5).

The LISA maps of *FRAC_AM* in the years 2001 and 2011 (Fig. 16a and Fig. 16b) present the statistically significant clusters and outliers. These maps reveal that high *FRAC_AM* clusters (dark red) were located mainly in the suburbs while low *FRAC_AM* clusters (dark blue) were located in the southern part of City District. This indicates that green spaces in these suburban sections were generally more complex-shaped than those in southern part of City District. This was due to the sparse green cover in the southern sections of City District in form of isolated single pixel patches. However, these suburban sections had relatively copious and continuous green cover, giving rise to complex patches. Further, a comparison of these two maps reveals two key aspects: i) the western suburbs lost large extent of high *FRAC_AM* clusters (dark red) in 2011, and ii) the northern part of City District emerged as hotspot of high *FRAC_AM* (dark red) in 2011. The former was an outcome of the severe reduction in green cover in the western suburbs that turned large green patches into several simple-shaped fragments. Concerning the latter, it was observed that this area witnessed augmentation of green spaces (see Fig. 6c) mainly along roads and railway lines, eventually leading to increased shape complexity.

The mean change in *FRAC_AM* of all census sections was 0. Relative to this mean, the LISA map of change in *FRAC_AM* (Fig. 16c) describes the census sections as ‘high’ (values from 0 to +0.13) and ‘low’ (values from -0.17 to 0). The map identifies the specific sections in western suburbs (dark blue) whose green spaces transformed into simple patches. The map also identifies the sections (dark red), mostly in the northern part of City District, whose green spaces turned more complex-shaped.

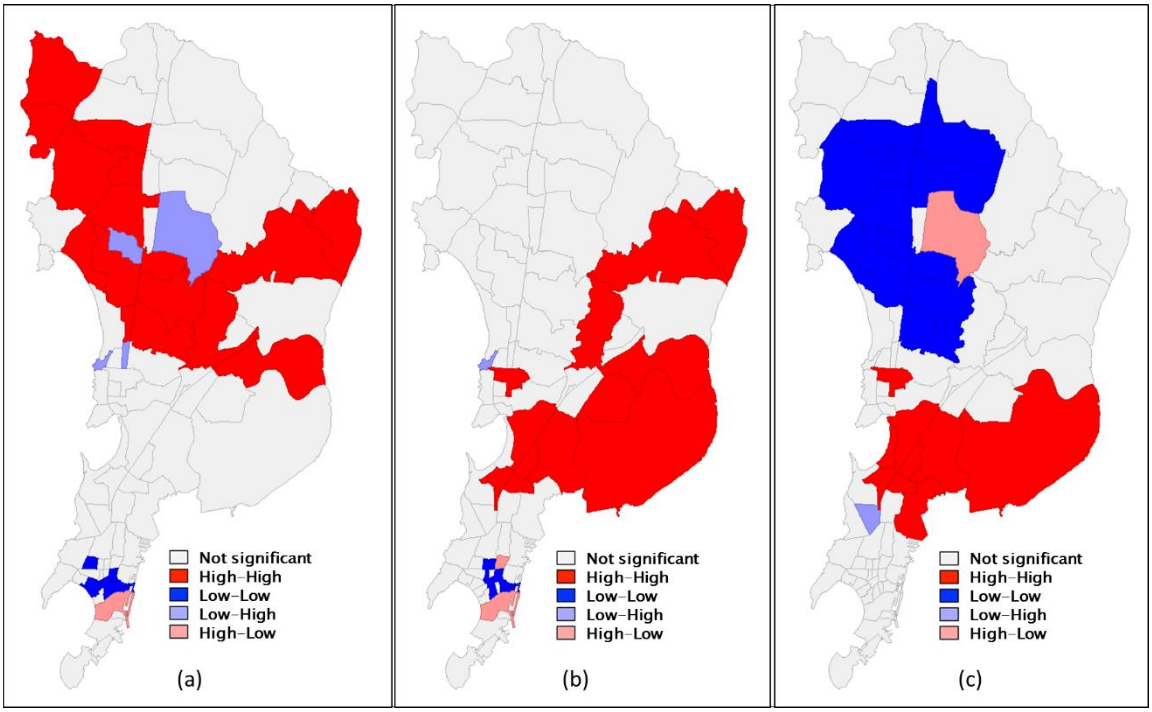

Fig. 16. LISA maps of (a) *FRAC_AM* in 2001, (b) *FRAC_AM* in 2011, and (c) change in *FRAC_AM* during 2001-11.

4.3.7 *Aggregation index of urban green space patches (AI)*

The *AI* of census sections ranged from 0 to 100% in 2001 and from 14.29 to 100% in 2011 (Table 5). The *AI* maps of census sections in 2001 and 2011 (Fig. 17a and Fig. 17b) reveal that most census sections witnessed disaggregation of their green spaces in the study period. Further, the median *AI* was observed to have decreased by 10.16 percentage points between 2001 and 2011 (Table 5). The change in *AI* during the study period was in the range of -34.54 percentage points (census section 58) to +13.64 percentage points (census section 11). The map of change in *AI* (Fig. 17c) reveals that all but one of the census sections experienced a decrease in *AI*. The census section 11 had shown an increased *AI* as it lost one of its only two green space patches. The widespread decrease in *AI* confirms that green spaces in Mumbai predominantly disaggregated during 2001-11. Further, as the results suggest, even in those sections that witnessed an increase in *PUGS*, the added green spaces were scattered and removed from the existing ones.

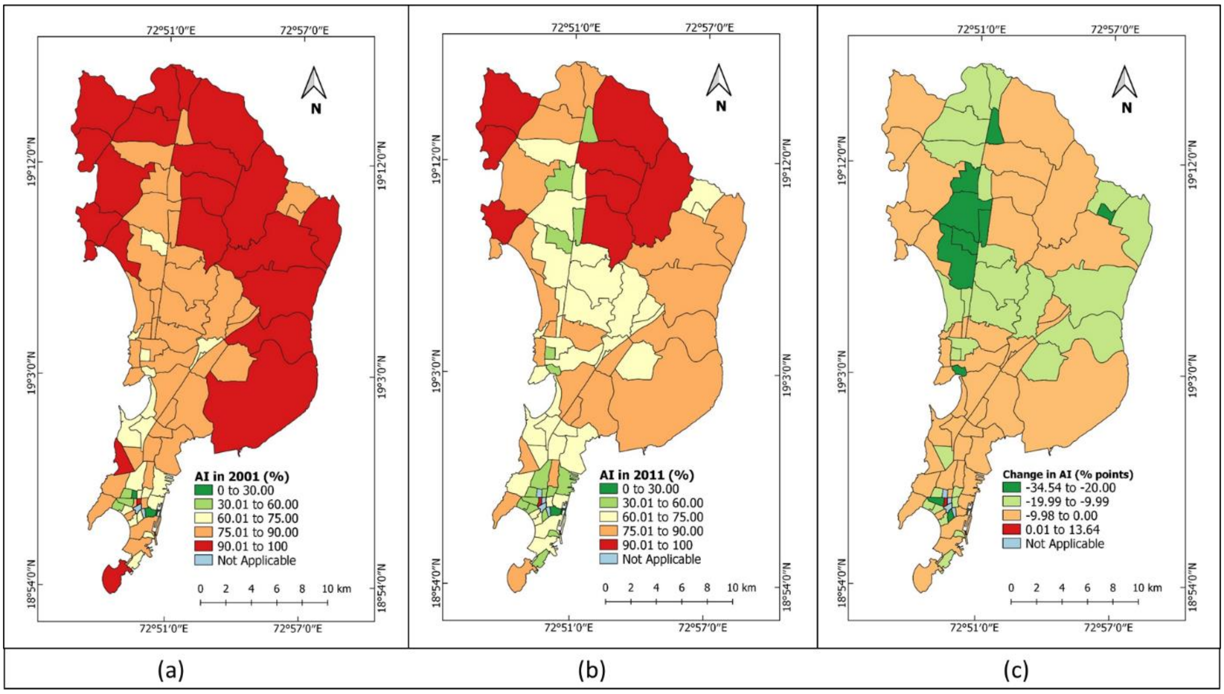

Fig. 17. Map of (a) *AI* in 2001, (b) *AI* in 2011, and (c) change in *AI* during 2001-11.

Note: The census sections with fewer than two green space pixels are represented as 'Not Applicable' in the maps (refer footnotes under Table 5).

The LISA maps of *AI* in the years 2001 and 2011 (Fig. 18a and Fig. 18b) present the statistically significant clusters and outliers. In both years, the southern sections of City District formed clusters of low *AI* (dark blue) as they had scant green cover distributed in form of few small patches. On the other hand, the suburbs contained clusters of high *AI* (dark red) since they had relatively abundant green cover in form of large lumps. However, as evident from a comparison of the two maps, the western suburbs lost substantial portions of high *AI* hotspots (dark red) between 2001 and 2011 due to extensive clearing of green spaces.

The mean change in *AI* of all census sections was -9.99 percentage points. Relative to this mean, the LISA map of change in *AI* (Fig. 18c) defines the census sections as 'high' (values from -9.99 to +13.64) and low (values from -34.54 to -9.99). This map identifies the census sections numbered 52, 56, 57 and 60 (dark blue) and their neighbours as hotspots of significant decline in *AI* during the study period. Further, the map shows that the disaggregation was relatively minimal around the Sanjay Gandhi National Park and sections 25 and 30 in the City District (dark red).

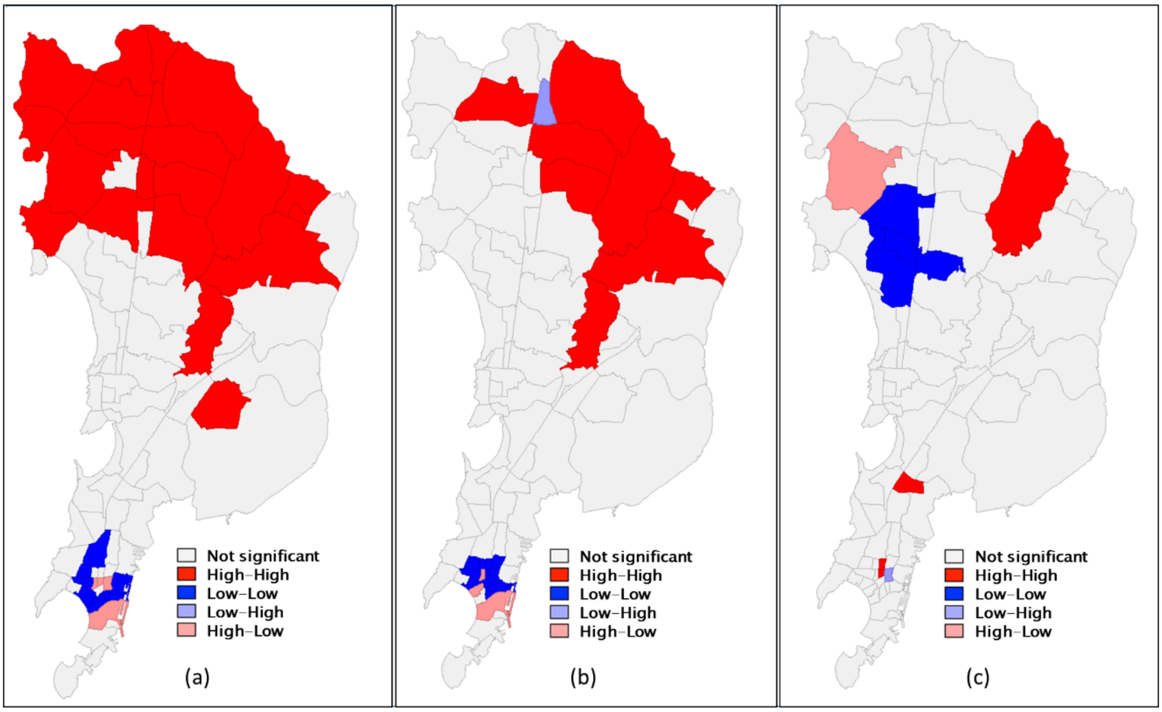

Fig. 18. LISA maps of (a) *AI* in 2001, (b) *AI* in 2011, and (c) change in *AI* during 2001-11.

5. Discussion and Conclusion

The study demonstrated a spatiotemporal analysis of urban green space distribution at neighbourhood level by adopting a novel geospatial approach. This approach encompasses quantity, quality and accessibility dimensions of green space distribution in order to provide a holistic assessment of green space dynamics, as recommended by *Yao et al. (2014), Haaland and van den Bosch (2015),* and *De la Barrera et al. (2016b).*

The study results indicate that green spaces in Mumbai overall diminished, fragmented, and disaggregated between 2001 and 2011. These results corroborate with the trends of urban green space decadence witnessed by other cities in the developing world, such as Dhaka (Bangladesh), Karachi (Pakistan), Hanoi (Vietnam) and Mashad (Iran), as reported by *Haaland and van den Bosch (2015).* The general degradation of urban green spaces in these cities could be attributed to multiple factors- spontaneous urbanization, poor land use management and general apathy to urban green space planning (*Byomkesh et al., 2012; Senanayake et al., 2013; Kabisch et al., 2015*). With Mumbai projected to become the world's sixth most populous city by 2028 (*UN DESA, 2018*), an urban greening policy framework with adequate measures for conserving and promoting urban green spaces against development pressure is the need of the hour.

The spatiotemporal analysis of neighbourhood level green space quantity indicators identified the hotpots of the greening and un-greening phenomena in Mumbai. The western suburbs, particularly the northern half, witnessed extreme levels of un-greening with much of its green spaces disappearing by 2011. The decrease in green cover in these neighbourhoods was simultaneous with their emergence as hub of residential and commercial development activities during this period (*Pethe et al., 2014*). The widely unabated urbanization of the western suburbs poses a threat to the ecologically sensitive verdant areas in the region, such as mangroves and the Sanjay Gandhi National Park, whose destruction has several adverse ramifications for the city and its residents (*Zerah, 2007; Vaz, 2014*). Similarly, the closely packed southern neighbourhoods of City District were found to have little to sparse green cover. However, these sections experienced relatively less decrease in green cover vis-à-vis the western suburbs. The population decrease fuelled by gentrification in these areas (*Pacione, 2006*) resulted in improved green space per capita (*UPI*) in few sections despite their diminishing green cover. Yet, remarkably, a few sections still reported decreased *UPI* in spite of decrease in population. This suggests that the further reduction of even meagre green spaces in these areas is driven by commercial development. On the other end of the gamut, the un-greening of Mumbai during the study period was comparatively less pronounced in the northern sections of City District. Interestingly, two census sections in this area (numbered 32 and 33) witnessed augmentation of green spaces despite their increasing population, and hence present a case for further research.

Furthermore, as evident from the spatiotemporal patterns of green space quality indicators, certain neighbourhoods in the western suburbs were also the foci of green space fragmentation phenomenon in Mumbai during 2001-11. Green spaces in these neighbourhoods witnessed sharp reduction in area and emerged increasingly distant from each other. Clearly these neighbourhoods deserve more attention in order to check their deteriorating quality of green spaces. On the other hand, the southern neighbourhoods in City District witnessed comparatively little fragmentation than the western suburbs between 2001 and 2011. However, the sparse green cover in these neighbourhoods were also observed to be distributed in form of isolated small patches. Hence, these neighbourhoods critically need greening programs to increase both their greenspace quantity and quality.

The spatiotemporal patterns of the green space accessibility indicators suggest that green spaces in most neighbourhoods turned relatively complex-shaped and disaggregated. This indicates that green spaces were increasingly proximate and, hence, more accessible to the residents. However, in the context of the extensive decrease and fragmentation of green spaces observed across Mumbai, the enhanced accessibility could be attributed to increased population settlements among fragmented green spaces rather than addition of green spaces. Further, we observed that in few neighbourhoods (e.g., census sections 52, 57, 58, 60 and 62), large and aggregated green space patches had turned into isolated single-pixel patches due to intense fragmentation (Figs. 3, 4). As a result, these neighbourhoods had disaggregated yet simple-shaped green space patches (Figs. 16c and 17c). Hence, accessibility to green spaces in these neighbourhoods cannot be inferred with certainty. This could be overcome if the variations in shape complexities are mapped at finer spatial resolutions.

The current study has a few limitations. First, the spatial heterogeneity within the census sections in terms of population and green space distribution could not be addressed as the census sections are the basic level of population data available publicly. Hence, the population is assumed to live at the centre of census section and access only the green spaces within the section (*Sathyakumar et al., 2018*). Second, the study is based on spatial metrics derived from remotely sensed data at 30m spatial resolution. Since the spatial metrics are scale-dependent (*Shen et al., 2004; Buyantuyev et al., 2010*), the distribution indicators evaluated in this study must be read in the context of the spatial resolution used.

Nevertheless, the study has significant implications for green space planning. As the distribution indicators are derived from remote sensing data, the analysis can be replicated in a cost effective manner at desired time scales to generate an inventory of neighbourhood-level green space distribution indicators. This would be particularly useful in case of cities in the developing countries that exhibit high urban dynamism spatially and temporally. Further, the statistical design provided by the study will help planners, especially in developing countries, to identify the neighbourhoods that deserve special attention. This paves way for planners in these countries to draw up local greening policies through efficient use of limited resources for improving the distributional equity of green spaces. Besides, the various distribution indicators thus derived can be coupled with green space function, neighbourhood pollution levels, socio-economic status, residents' perceptions and preferences to build a multi-pronged approach towards urban greening (*Lo and Jim, 2012; Wright Wendel et al., 2012; Senanayake et al., 2013; Sathyakumar et al., 2018*). Further, future studies can contemplate independently assessing the distribution of green spaces according to their ownership (public/private owned) or hierarchical levels (neighbourhood-level/community-level/district-level/city-level parks) (*Li and Liu, 2016; Gupta et al., 2016*). Moreover, replicating the study for other cities may help in formulating urban green quality and accessibility standards in addition to the existing quantity standards (*Haaland and van den Bosch, 2015; Badiu et al., 2016*). However, a key element to be considered while making inter-city or multi-scale comparison of the remote sensing-derived indicators is the homogeneous spatial resolution of the satellite images used (*Sathyakumar et al., 2018*).

Declaration

Conflicts of interest: none.

This research did not receive any specific grant from funding agencies in the public, commercial, or not-for-profit sectors.

Appendix A. Conventional error matrices of the UGS maps of Mumbai in 2001 and 2011.

Table A1
Conventional error matrix of the urban green spaces (UGS) map of Mumbai in 2001.

Map	Reference		Total	User's Accuracy
	UGS	Non-UGS		
UGS	208	31	239	87.03 %
Non-UGS	16	145	161	90.06 %
Total	224	176	400	
Producer's Accuracy	92.86 %	82.39 %		

Overall accuracy= 88.25 % Kappa= 0.76

Table A2
Conventional error matrix of the urban green spaces (UGS) map of Mumbai in 2011.

Map	Reference		Total	User's Accuracy
	UGS	Non-UGS		
UGS	164	30	194	84.54 %
Non-UGS	38	168	206	81.55 %
Total	202	198	400	
Producer's Accuracy	81.19 %	84.85 %		

Overall accuracy= 83.00 % Kappa= 0.66

References

Anguluri, R., & Narayanan, P. (2017). Role of green space in urban planning: Outlook towards smart cities. *Urban Forestry and Urban Greening*, *25*, 58–65. http://doi.org/10.1016/j.ufug.2017.04.007

Anselin, L. (1995). Local Indicators of Spatial Association - LISA. *Geographical Analysis*, 27(2), 93–115. http://doi.org/10.1111/j.1538-4632.1995.tb00338.x

Badiu, D. L., Ioja, C. I., Patroescu, M., Breuste, J., Artmann, M., Niţa, M. R., Onose, D. A. (2016). Is urban green space per capita a valuable target to achieve cities' sustainability goals? Romania as a case study. *Ecological Indicators*, *70*, 53–66. http://doi.org/10.1016/j.ecolind.2016.05.044

Bardhan, R., Sarkar, S., Jana, A., & Velaga, N.R. (2015a). Mumbai slums since independence: Evaluating the policy outcomes. *Habitat International*, 50, 1–11. http://doi.org/10.1016/j.habitatint.2015.07.009

Bardhan, R., Kurisu, K., & Hanaki, K. (2015b). Does compact urban forms relate to good quality of life in high density cities of India? Case of Kolkata. *Cities*, 48, 55–65. http://doi.org/10.1016/j.cities.2015.06.005

Bardhan, R., Debnath, R., & Bandopadhyay, S. (2016). A conceptual model for identifying the risk susceptibility of urban green spaces using geo-spatial techniques. *Modeling Earth Systems and Environment*, 2(3), 144. https://doi.org/10.1007/s40808-016-0202-y

Baud, I., Kuffer, M., Pfeffer, K., Sliuzas, R., & Karuppannan, S. (2010). Understanding heterogeneity in metropolitan India: The added value of remote sensing data for analyzing substandard residential areas. *International Journal of Applied Earth Observation and Geoinformation*, 12(5), 359–374. http://doi.org/10.1016/j.jag.2010.04.008

Buyantuyev, A., Wu, J., & Gries, C. (2010). Multiscale analysis of the urbanization pattern of the Phoenix metropolitan landscape of USA: Time, space and thematic resolution. *Landscape and Urban Planning*, 94(3–4), 206–217. http://doi.org/10.1016/j.landurbplan.2009.10.005

Byomkesh, T., Nakagoshi, N., & Dewan, A. M. (2012). Urbanization and green space dynamics in Greater Dhaka, Bangladesh. *Landscape and Ecological Engineering*, *8*(1), 45–58. http://doi.org/10.1007/s11355-010-0147-7

Census FPT (2001). *Census of India 2001: Final Population Totals* [Data file]. Office of Register General and Census Commissioner of India. Available from http://www.censusindia.gov.in/DigitalLibrary/Tables.aspx Accessed 04.04.2018.

Census PCA (2011). *Census of India 2011: Primary Census Abstract* [Data file]. Office of Register General and Census Commissioner of India. Available from http://censusindia.gov.in/pca/pcadata/pca.html Accessed 19.07.2017.

CEO Maharashtra (2017). Maps of Assembly Constituencies. Available from https://ceo.maharashtra.gov.in/maplinks/maps.aspx Accessed 19.07.2017.

De la Barrera, F., Reyes-Paecke, S., Harris, J., Bascunan, D., & Farias, J. M. (2016a). People's perception influences on the use of green spaces in socio-economically differentiated neighborhoods. *Urban Forestry and Urban Greening*, 20, 254–264. http://doi.org/10.1016/j.ufug.2016.09.007

De la Barrera, F., Reyes-Paecke, S., & Banzhaf, E. (2016b). Indicators for green spaces in contrasting urban settings. *Ecological Indicators*, *62*, 212–219. http://doi.org/10.1016/j.ecolind.2015.10.027

De Satgé, R., & Watson, V. (2018). *Urban Planning in the Global South*. *Urban Planning in the Global South*. http://doi.org/10.1007/978-3-319-69496-2

Du Toit, M. J., Cilliers, S. S., Dallimer, M., Goddard, M., Guenat, S., & Cornelius, S. F. (2018). Urban green infrastructure and ecosystem services in sub-Saharan Africa. *Landscape and Urban Planning*, http://doi.org/10.1016/j.landurbplan.2018.06.001

Fernández, I. C., & Wu, J. (2016). Assessing environmental inequalities in the city of Santiago (Chile) with a hierarchical multiscale approach. *Applied Geography*, 74, 160–169. http://doi.org/10.1016/j.apgeog.2016.07.012

Franco, S. F., & Macdonald, J. L. (2017). Measurement and valuation of urban greenness: Remote sensing and hedonic applications to Lisbon, Portugal. *Regional Science and Urban Economics*, *72*, *156-180*. http://doi.org/10.1016/j.regsciurbeco.2017.03.002

Gascon, M., Cirach, M., Martinez, D., Dadvand, P., Valentin, A., Plasencia, A., & Nieuwenhuijsen, M. J. (2016). Normalized difference vegetation index (NDVI) as a marker of surrounding greenness in epidemiological studies: The case of Barcelona city. *Urban Forestry and Urban Greening*, 19, 88–94. http://doi.org/10.1016/j.ufug.2016.07.001

GeoDa (2019). An Introduction to Spatial Data Analysis: Local Spatial Autocorrelation. Retrieved from https://geodacenter.github.io/workbook/6a_local_auto/lab6a.html Accessed 22.08.2019.

Gupta, K., Kumar, P., Pathan, S. K., & Sharma, K. P. (2012). Urban neighbourhood green index- A measure of green spaces in urban areas. *Landscape and Urban Planning*, 105(3), 325–335. http://doi.org/10.1016/j.landurbplan.2012.01.003

Gupta, K., Roy, A., Luthra, K., Maithani, S., & Mahavir. (2016). GIS based analysis for assessing the accessibility at hierarchical levels of urban green spaces. *Urban Forestry and Urban Greening*, *18*, 198–211. http://doi.org/10.1016/j.ufug.2016.06.005

Haaland, C., & van den Bosch, C. K. (2015). Challenges and strategies for urban green-space planning in cities undergoing densification: A review. *Urban Forestry and Urban Greening*, *14*(4), 760–771. http://doi.org/10.1016/j.ufug.2015.07.009

Heynen, N., Perkins, H. A., & Roy, P. (2006). The political ecology of uneven urban green space. *Urban Affairs Review*, 42(1), 3–25. http://doi.org/10.1177/1078087406290729

Hughey, S. M., Kaczynski, A. T., Porter, D. E., Hibbert, J., Turner-McGrievy, G., & Liu, J. (2018). Spatial clustering patterns of child weight status in a southeastern US county. *Applied Geography*, 99, 12–21. http://doi.org/10.1016/j.apgeog.2018.07.016

Jim, C. Y. (2013). Sustainable urban greening strategies for compact cities in developing and developed economies. *Urban Ecosystems*, *16*(4), 741–761. http://doi.org/10.1007/s11252-012-0268-x

Kabisch, N., Qureshi, S., & Haase, D. (2015). Human-environment interactions in urban green spaces - A systematic review of contemporary issues and prospects for future research. *Environmental Impact Assessment Review*, 50, 25–34. http://doi.org/10.1016/j.eiar.2014.08.007

Li, H., & Liu, Y. (2016). Neighborhood socioeconomic disadvantage and urban public green spaces availability: A localized modeling approach to inform land use policy. *Land Use Policy*, 57, 470–478. http://doi.org/10.1016/j.landusepol.2016.06.015

Lin, B., Meyers, J., & Barnett, G. (2015). Understanding the potential loss and inequities of green space distribution with urban densification. *Urban Forestry & Urban Greening*, 14, 952-958. http://dx.doi.org/10.1016/j.ufug.2015.09.003

Lo, A. Y. H., & Jim, C. Y. (2012). Citizen attitude and expectation towards greenspace provision in compact urban milieu. *Land Use Policy*, 29(3), 577–586. http://doi.org/10.1016/j.landusepol.2011.09.011

Maktav, D., Erbek, F. S., & Jürgens, C. (2005). Remote sensing of urban areas. *International Journal of Remote Sensing*, *26*(4), 655–659. http://doi.org/10.1080/01431160512331316469

McGarigal, K., Cushman, S.A., & Ene, E. (2012). FRAGSTATS : Spatial Pattern Analysis Program for Categorical and Continuous Maps (Version 4.2) [Software]. Available from http://www.umass.edu/landeco/research/fragstats/fragstats.html Accessed 19.07.2017.

McGarigal, K. (2015). FRAGSTATS Help. Retrieved from http://www.umass.edu/landeco/research/fragstats/documents/fragstats.help.4.2.pdf Accessed 19.07.2017.

MCGM. (2016). Report of Draft Development Plan-2034. Mumbai: Municipal Corporation of Greater Mumbai.

Mehrotra, S., Bardhan, R., & Ramamritham, K. (2018). Urban Informal Housing and Surface Urban Heat Island Intensity: Exploring Spatial Association in the City of Mumbai. Environment and Urbanization ASIA, 9(2), 158–177. https://doi.org/10.1177/0975425318783548

Mehrotra, S., Bardhan, R., & Ramamritham, K. (2019). Outdoor thermal performance of heterogeneous urban environment: An indicator-based approach for climate-sensitive planning. *Science of the Total Environment*. https://doi.org/10.1016/j.scitotenv.2019.03.152

Nero, B. F. (2017). Urban green space dynamics and socio-environmental inequity: multi-resolution and spatiotemporal data analysis of Kumasi, Ghana, *International Journal of Remote Sensing*, 38:23, 6993-7020, https://doi.org/10.1080/01431161.2017.1370152

O'Malley, C., Piroozfar, P., Farr, E. R. P., & Pomponi, F. (2015). Urban Heat Island (UHI) mitigating strategies: A case-based comparative analysis. *Sustainable Cities and Society*, *19*, 222–235. http://doi.org/10.1016/j.scs.2015.05.009

Otsu, N. (1979). A threshold selection method from gray-level histograms. *IEEE Transactions on Systems, Man, and Cybernetics*, 9(1), 62–66.

Pacione, M. (2006). Mumbai. *Cities*, 23(3), 229–238. http://doi.org/10.1016/j.cities.2005.11.003

Pethe, A., Nallathiga, R., Gandhi, S., & Tandel, V. (2014). Re-thinking urban planning in India: Learning from the wedge between the de jure and de facto development in Mumbai. *Cities*, 39, 120–132. http://doi.org/10.1016/j.cities.2014.02.006

Pham, T. T. H., Apparicio, P., Séguin, A. M., Landry, S., & Gagnon, M. (2012). Spatial distribution of vegetation in Montreal: An uneven distribution or environmental inequity? *Landscape and Urban Planning*, *107*(3), 214–224. http://doi.org/10.1016/j.landurbplan.2012.06.002

QGIS (2019). QGIS Python Plugins Repository- QuickMapServices. Available from https://plugins.qgis.org/plugins/quick_map_services/ Accessed 18.08.2019.

Qian, Y., Zhou, W., Yu, W., & Pickett, S. T. A. (2015). Quantifying spatiotemporal pattern of urban greenspace : new insights from high resolution data. *Landscape Ecology*, 1165–1173. http://doi.org/10.1007/s10980-015-0195-3

Rigolon, A., Browning, M., & Jennings, V. (2018). Inequities in the quality of urban park systems: An environmental justice investigation of cities in the United States. *Landscape and Urban Planning*, 178, 156–169. http://doi.org/10.1016/j.landurbplan.2018.05.026

Sathyakumar, V., Ramsankaran, R. A. A. J., & Bardhan, R. (2018). Linking remotely sensed Urban Green Space (UGS) distribution patterns and Socio-Economic Status (SES) - A multi-scale probabilistic analysis based in Mumbai, India. *GIScience and Remote Sensing*. http://doi.org/10.1080/15481603.2018.1549819

Senanayake, I.P., Welivitiya, W. D. D. P., & Nadeeka, P. M. (2013). Urban green spaces analysis for development planning in Colombo, Sri Lanka, utilizing THEOS satellite imagery– A remote sensing and GIS approach. *Urban Forestry & Urban Greening*, 12, 307-314. http://dx.doi.org/10.1016/j.ufug.2013.03.011

Shafizadeh Moghadam, H., & Helbich, M. (2013). Spatiotemporal urbanization processes in the megacity of Mumbai, India: A Markov chains-cellular automata urban growth model. *Applied Geography*, *40*, 140–149. http://doi.org/10.1016/j.apgeog.2013.01.009

Shekhar, S. & Aryal, J. (2019). Role of geospatial technology in understanding urban green space of Kalaburagi city for sustainable planning. *Urban Forestry & Urban Greening*, 46, 126450. https://doi.org/10.1016/j.ufug.2019.126450

Shen, W, Jenerette, G. D., Wu, J., & Gardner, R. H. (2004). Evaluating empirical scaling relations of pattern metrics with simulated landscapes. *Ecography*, 27(4): 459-469.

Singh, K. K. (2018). Urban green space availability in Bathinda City, India. *Environmental Monitoring and Assessment*, 190: 671. https://doi.org/10.1007/s10661-018-7053-0

Stehman, S.V., & Foody, G.M. (2019). Key issues in rigorous accuracy assessment of land cover products. *Remote Sensing of Environment*, 231, 111199. https://doi.org/10.1016/j.rse.2019.05.018

Sunder, S., Ramsankaran, R., & Ramakrishnan, B. (2017). Inter-comparison of remote sensing sensing-based shoreline mapping techniques at different coastal stretches of India. *Environmental Monitoring and Assessment*, 189: 290. http://doi.org/10.1007/s10661-017-5996-1

Tian, Y., Jim, C. Y., & Wang, H. (2014). Assessing the landscape and ecological quality of urban green spaces in a compact city. *Landscape and Urban Planning*, *121*, 97–108. http://doi.org/10.1016/j.landurbplan.2013.10.001

United Nations Department of Economic and Social Affairs (UN DESA), 2018. The World Cities in 2018- Data Booklet. Retrieved from https://www.un.org/en/development/desa/population/publications/pdf/urbanization/the_worlds_cities_in_2018_data_booklet.pdf Accessed 06.05.2019.

United Nations Population Fund (UNPF), 2007. State of world population 2007: Unleashing the Potential of Urban Growth. Retrieved from http://www.unfpa.org/swp/ Accessed 06.12.2017.

Vaz, E. (2014). Managing urban coastal areas through landscape metrics: An assessment of Mumbai's mangrove system. *Ocean & Coastal Management, 98, 27-37.* https://doi.org/10.1016/j.ocecoaman.2014.05.020

Wright Wendel, H. E., Zarger, R. K., & Mihelcic, J. R. (2012). Accessibility and usability: green space preferences, perceptions, and barriers in a rapidly urbanizing city in Latin America. *Landscape and Urban Planning*, 107(3), 272–282. http://dx.doi.org/10.1016/j.landurbplan.2012.06.003

Yao, L., Liu, J., Wang, R., Yin, K., & Han, B. (2014). Effective green equivalent - A measure of public green spaces for cities. *Ecological Indicators*, *47*, 123–127. http://doi.org/10.1016/j.ecolind.2014.07.009

You, H. (2016). Characterizing the inequalities in urban public green space provision in Shenzhen, China. *Habitat International*, 56, 176–180. http://doi.org/10.1016/j.habitatint.2016.05.006

Zérah, M. H. (2007). Conflict between green space preservation and housing needs: The case of the Sanjay Gandhi National Park in Mumbai. *Cities*, *24*(2), 122–132. http://doi.org/10.1016/j.cities.2006.10.005

Zhang, C., Luo, L., Xu, W., Ledwith, V. (2008). Use of local Moran's I and GIS to identify pollution hotspots of Pb in urban soils of Galway, Ireland. *Science of the Total Environment, 398, 212-221.* https://doi.org/10.1016/j.scitotenv.2008.03.011

Zhou, X., & Kim, J. (2013). Social disparities in tree canopy and park accessibility: A case study of six cities in Illinois using GIS and remote sensing. *Urban Forestry and Urban Greening*, *12*(1), 88–97. http://doi.org/10.1016/j.ufug.2012.11.004

Zhou, X., & Wang, Y. (2011). Spatial–temporal dynamics of urban green space in response to rapid urbanization and greening policies. *Landscape and Urban Planning*, 100, 268–277. http://doi:10.1016/j.landurbplan.2010.12.013

Zhou, W., Wang, J., Qian, Y., Pickett, S. T. A., Li, W., & Han, L. (2018). The rapid but "invisible" changes in urban greenspace: A comparative study of nine Chinese cities. *Science of the Total Environment*, 627, 1572–1584. http://doi.org/10.1016/j.scitotenv.2018.01.335s